

REPORT 1225
 (II) of 11
 (II) of 11
 (II) of 11

REPORT 1225

DETERMINATION OF LATERAL-STABILITY DERIVATIVES AND TRANSFER-FUNCTION COEFFICIENTS FROM FREQUENCY-RESPONSE DATA FOR LATERAL MOTIONS¹

By JAMES J. DONEGAN, SAMUEL W. ROBINSON, JR., and ORRIN W. GATES, JR.

SUMMARY

A method is presented for determining the lateral-stability derivatives, transfer-function coefficients, and the modes for lateral motion from frequency-response data for a rigid aircraft. The method is based on the application of the vector technique to the equations of lateral motion, so that the three equations of lateral motion can be separated into six equations. The method of least squares is then applied to the data for each of these equations to yield the coefficients of the equations of lateral motion from which the lateral-stability derivatives and lateral-motion transfer-function coefficients are computed. Two numerical examples are given to demonstrate the use of the method.

INTRODUCTION

In the reduction and generalization of flight-test data, whether for loads, stability, or control purposes, the airplane stability derivatives and the coefficients of the transfer functions are often required. A great deal of emphasis, therefore, has been placed on the development of analytical methods for reducing flight data to obtain these basic derivatives and coefficients.

A number of recent methods, for example references 1 to 4, are now available for analyzing longitudinal maneuvers and determining the longitudinal-stability derivatives and transfer-function coefficients from flight data. References 1 and 2 present methods of determining the longitudinal-stability derivatives and transfer functions directly from transient data. Reference 3 reduces data for longitudinal motion determined from the forced-oscillation technique by means of circle diagrams to longitudinal-stability derivatives and frequency response. Mueller, in reference 5, was one of the earliest to use vector representation in the equations of longitudinal motion to represent the derivatives and integrals of the variables. Schumacher, reference 4, represented the frequency responses to longitudinal motion as vectors and substituted them into the equations of longitudinal motion and the transfer functions. He then applied the method of least squares to these vector equations, a method which he found very effective in determining certain of the longitudinal-stability derivatives and transfer-function coefficients.

The problem of analyzing lateral motions, however, has not received the same amount of attention as that for longitudinal motion, perhaps because it is more complicated. Several analytical investigations have been undertaken and a

few methods have been proposed such as the circle-diagram method (ref. 6), the step-function-response method (ref. 6) in which the response of an airplane to a step deflection of the rudder or aileron is analyzed, and the free-oscillation method (ref. 7) in which the period and damping of the free vibrations of the aircraft due to a pulse-type input are analyzed. Since the usefulness of these methods is limited by the number of derivatives which can be extracted, there is still a need for a more general method of analysis that will extract all the significant lateral-stability derivatives from flight data.

It is the purpose of this report to present a method for determining the lateral-stability derivatives of a rigid airplane and to illustrate its use by applying it to two examples. The method is based on the vector representation of the frequency responses to lateral motions. This vector approach permits separation of each of the equations of lateral motion into a real and imaginary equation. A least-squares method is then applied to the data in each of these equations or combinations thereof to yield the coefficients of the equations of lateral motion. The lateral-stability derivatives and transfer-function coefficients are then determined from these coefficients and the known aircraft mass parameters.

The method is applied to two specific examples, one in which the frequency responses to a rudder input are known and one in which the transient responses to aileron deflection are known. In the latter case, the frequency responses were obtained from the transient motions by two methods and the stability derivatives computed.

An attempt has been made to schedule the procedure so as to reduce the dependence of the results obtained from this method on the derivatives that can be least accurately obtained from the particular data being analyzed; however, further improvements may be made as further experience is gained in the application of the method.

SYMBOLS

| | |
|--|---|
| a_y | lateral acceleration, ft/sec ² |
| $A_\beta, A_\phi, A_\psi, A_{\dot{\beta}}, A_{\dot{\phi}}, A_{\dot{\psi}}, A_{\ddot{\beta}}, A_{\ddot{\phi}}, A_{\ddot{\psi}}$ | parameters defined by equations (8) |
| $B_\beta, B_\phi, B_\psi, B_{\dot{\beta}}, B_{\dot{\phi}}, B_{\dot{\psi}}, B_{\ddot{\beta}}, B_{\ddot{\phi}}, B_{\ddot{\psi}}$ | parameters defined by equations (9) |
| b | wing span, ft |
| C_L | lift coefficient, L/qS |
| $\bar{C}_L = \frac{W}{qS}$ | oldham coefficient |
| C_n | yawing-moment coefficient, N/qSb |

¹Supersedes NACA TN 3083, 1954.

| | | | |
|------------------------|--|--|--|
| C_l | rolling-moment coefficient, L'/qSb | V | true airspeed, ft/sec |
| C_Y | lateral-force coefficient, Lateral force/ qS | W | aircraft weight, lb |
| C_1, C_2, C_3 | coefficient of transfer functions (defined in table II) | X, Y, Z | airplane stability axes (see fig. 1) |
| D | differential operator, $\frac{d}{dt}$ | α | angle of attack, radians |
| e | natural logarithmic base | β | angle of sideslip, v/V , radians |
| F_1, F_2, F_3 | forcing-function coefficients representing rudder effectiveness (defined in table I) | δ_a | aileron control deflection, radians |
| G_2, G_3 | forcing-function coefficients representing aileron effectiveness (defined in table I) | δ_r | rudder control deflection, radians |
| g | acceleration due to gravity, ft/sec ² | η | inclination of principal longitudinal axis of inertia with respect to flight path (positive when the positive direction of the X principal axis is inclined above the flight path) |
| I_X | moment of inertia about stability X -axis, mk_X^2 , slug-ft ² | μ_b | nondimensional mass parameter used for lateral equations, $m/\rho S b$ |
| I_Z | moment of inertia about stability Z -axis, mk_Z^2 , slug-ft ² | ρ | air density, slugs/cu ft |
| I_{XZ} | product of inertia referred to stability axes (negative when the positive direction of the X principal axis is inclined above the flight path, i. e., when η is positive) | τ | time parameter, $m/\rho S V$, sec |
| $i=\sqrt{-1}$ | | Φ | phase angle, radians |
| K_1, K_2, K_3, \dots | stability-derivative coefficients of the equations of lateral motion (defined in table I) | ϕ | angle of roll, radians |
| k_X | radius of gyration about stability X -axis, ft | ψ | angle of yaw, radians |
| k_Z | radius of gyration about stability Z -axis, ft | ω | angular frequency, radians/sec |
| K_X | nondimensional radius of gyration about longitudinal stability axis, $\frac{\sqrt{(k_{x_0}/b)^2 \cos^2 \eta + (k_{x_0}/b)^2 \sin^2 \eta}}{b}$ | Bar notation: | |
| K_Z | nondimensional radius of gyration about vertical stability axis, $\frac{\sqrt{(k_{x_0}/b)^2 \cos^2 \eta + (k_{x_0}/b)^2 \sin^2 \eta}}{b}$ | \bar{q} | bar over letter represents maximum value |
| K_{XZ} | nondimensional product-of-inertia parameter, $-\frac{[(k_{x_0}/b)^2 - (k_{x_0}/b)^2] \cos \eta \sin \eta}{b^2}$ | $ a $ | bars on sides of symbol represent absolute value |
| k_{x_0} | radius of gyration about principal longitudinal axis, ft | Matrix notation: | |
| k_{z_0} | radius of gyration about principal vertical axis, ft | $[]$ | square matrix |
| L | lift, lb | $\{ \}$ | column matrix |
| L' | rolling moment, ft-lb | The lateral-stability derivatives are expressed by subscript notation as, for example: | |
| M | Mach number | $C_{l\beta} = \frac{\partial C_l}{\partial \beta}$, $C_{l\dot{\beta}} = \frac{\partial C_l}{\partial \frac{p b}{2V}}$, and $C_{l\dot{\gamma}} = \frac{\partial C_l}{\partial \frac{r b}{2V}}$ | |
| m | aircraft mass, W/g , slugs | ³ Phase angles are also indicated by subscript notation as $\Phi_{\beta\gamma}$, is the phase angle between the input rudder deflection and the output sideslip angle. | |
| N | yawing moment, ft-lb | DEVELOPMENT OF METHOD | |
| p or $\dot{\phi}$ | incremental rolling angular velocity about X -axis, radians/sec | EQUATIONS OF LATERAL MOTION | |
| q | dynamic pressure, $\frac{1}{2} \rho V^2$, lb/sq ft | The equations of lateral motion based on the stability axes (as shown in fig. 1) and on the usual assumptions of linearity, small angles, and maneuvers which start from a level-flight condition are usually written in the following form: | |
| r or $\dot{\psi}$ | incremental yawing angular velocity about Z -axis, radians/sec | (a) For the sideslipping motion, | |
| R | amplitude ratio | $(D + K_1)\beta - K_2\phi + D\psi = F_1\delta_r(t)$ (1) | |
| S | wing area, sq ft | or, since $a_y = V(D\beta + D\psi - K_2\phi)$, | |
| s | Laplace transform variable | $\frac{1}{V} a_y + K_1\beta = F_1\delta_r(t)$ (1a) | |
| t | time, sec | (b) For the rolling motion, | |
| v | incremental component of velocity V along the Y -axis, ft/sec | $K_3\beta + (D^2 + K_4D)\phi - (K_5D^2 + K_6D)\psi = F_2\delta_r(t) + G_2\delta_a(t)$ (2) | |
| | | (c) For the yawing motion, | |
| | | $-K_7\beta - (K_8D^2 + K_9D)\phi + (D^2 + K_{10}D)\psi = F_3\delta_r(t) + G_3\delta_a(t)$ (3) | |

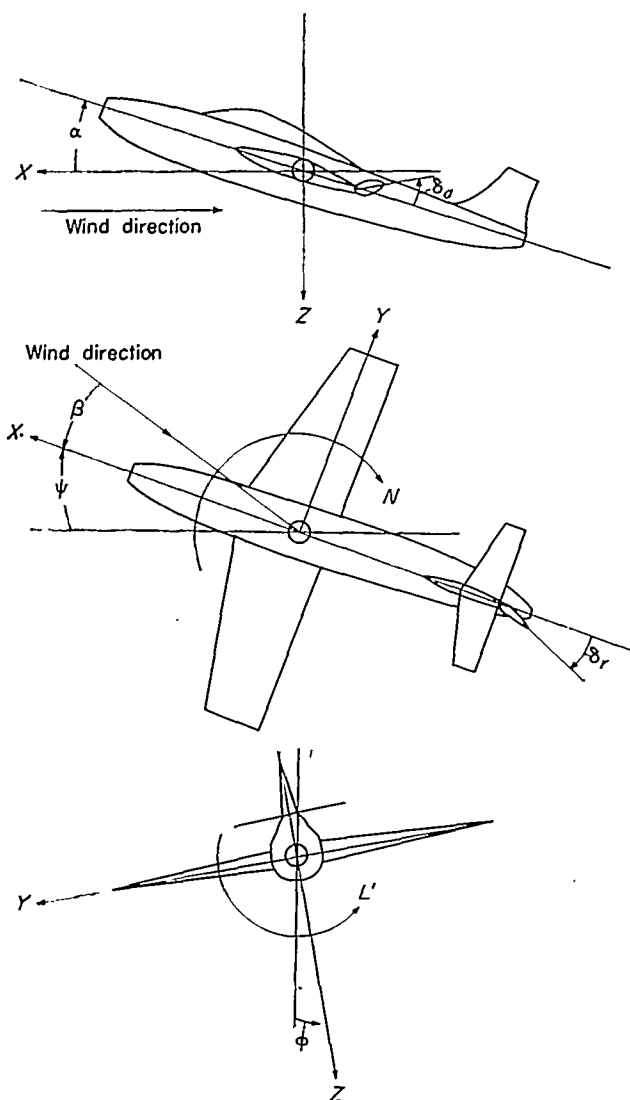


FIGURE 1.—Stability axis system showing positive directions.

where the K , F , and G coefficients are defined in table I. The forcing functions of these equations are written for rudder inputs and aileron inputs combined; for the sake of simplicity in developing and demonstrating the method, only rudder inputs $F_1\delta_r(t)$, $F_2\delta_r(t)$, and $F_3\delta_r(t)$ are considered. The method, however, applies equally well to both aileron and rudder inputs as is shown subsequently.

VECTOR INTERPRETATION OF FREQUENCY RESPONSE

In many current studies of airplane dynamics, the frequency response of the aircraft is determined from flight data. Having the data available in the frequency plane offers certain advantages over having the data in the time plane, since use can then be made of the vector interpretation of frequency response. The development which follows will assume that the data to be analyzed are available in frequency-response form. In the event that only transient-response data are available, the transformation to the frequency plane can be made from a selection of one of the several methods compared in reference 8.

The vector technique is applied to the determination of lateral-stability derivatives in the following manner. If an input δ_r to a linear system (a system described by a linear differential equation) is considered to have a sinusoidal vari-

TABLE I.—DEFINITIONS OF THE COEFFICIENTS OF THE EQUATIONS OF LATERAL MOTION OF AIRPLANE

| Stability-derivative coefficients: | Control-effectiveness coefficients: |
|--|---|
| $K_1 = C_{Y\beta} \left(-\frac{1}{2\tau} \right)$ | $F_1 = C_{Y\delta_r} \frac{1}{2\tau}$ |
| $K_2 = \bar{C}_L \frac{1}{2\tau} = g/V$ | $F_2 = C_{L\delta_r} \frac{\mu b}{2(k_X/b)^2 \tau^2}$ |
| $K_3 = C_{L\beta} \left[-\frac{\mu b}{2(k_X/b)^2 \tau^2} \right]$ | $F_3 = C_{L\delta_r} \frac{\mu b}{2(k_X/b)^2 \tau^2}$ |
| $K_4 = C_{Lp} \left[-\frac{1}{4\tau(k_X/b)^2} \right]$ | $G_2 = C_{L\delta_a} \frac{\mu b}{2(k_X/b)^2 \tau^2}$ |
| $K_5 = I_{XZ}/I_X$ | $G_3 = C_{N\delta_a} \frac{\mu b}{2(k_Z/b)^2 \tau^2}$ |
| $K_6 = C_{Lr} \frac{1}{4\tau(k_X/b)^2}$ | |
| $K_7 = C_{N\beta} \frac{\mu b}{2(k_Z/b)^2 \tau^2}$ | |
| $K_8 = I_{XZ}/I_Z$ | |
| $K_9 = C_{Nr} \frac{1}{4\tau(k_Z/b)^2}$ | |
| $K_{10} = C_{nr} \left[-\frac{1}{4\tau(k_Z/b)^2} \right]$ | |

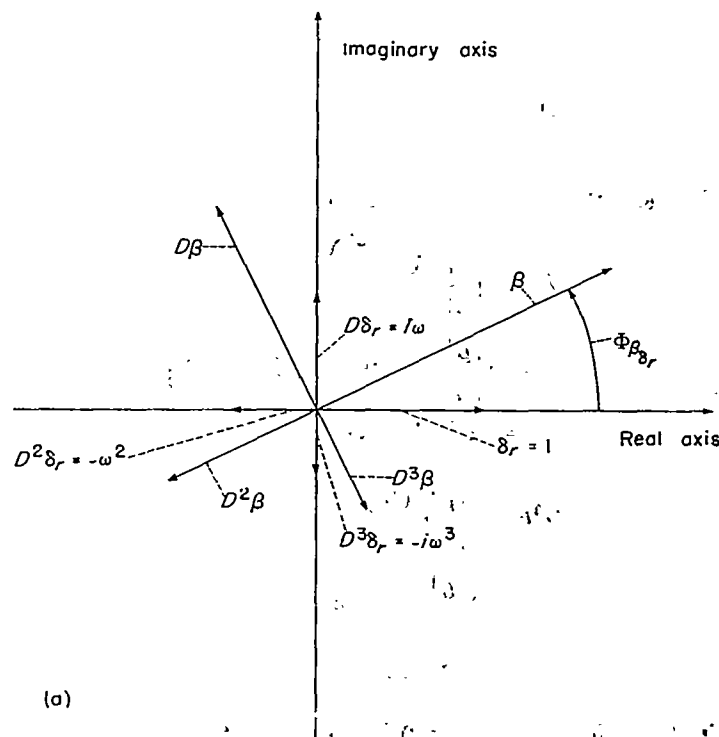
(a) Vector diagram showing relative magnitudes and positions of input δ_r and output β , and their derivatives. $\omega = 0.7$ radian/sec.

FIGURE 2.—Vector representation of lateral variables.

ation of frequency ω , it can be considered to be a vector of unit magnitude lying along the real axis of the complex plane as shown in figure 2(a). The first derivative of the sinusoidal input $D\delta_r$ is then obtained by multiplying the amplitude by ω and rotating the resulting vector 90° counterclockwise in the complex plane which is equivalent to advancing the phase angle by 90° . Each succeeding higher derivative is found by multiplying by ω and rotating the vector 90° in

the complex plane; thus,

$$\delta_r = 1 \quad (4)$$

$$D\delta_r = i\omega \quad (5)$$

$$D^2\delta_r = -\omega^2 \quad (6)$$

The steady-state output or response of the linear system to a sinusoidal input may be considered to be a vector of magnitude equal to an amplitude ratio R and having a direction angularly displaced from the real axis by a phase angle Φ . Thus, in the complex plane, the vector for sideslip may be represented as

$$\beta = \left| \frac{\bar{\beta}}{\delta_r} \right| e^{i\Phi_{\beta\delta_r}} = \left| \frac{\bar{\beta}}{\delta_r} \right| (\cos \Phi_{\beta\delta_r} + i \sin \Phi_{\beta\delta_r}) = A_\beta + iB_\beta \quad (7)$$

By definition,

$$\left. \begin{aligned} A_\beta &= \left| \frac{\bar{\beta}}{\delta_r} \right| \cos \Phi_{\beta\delta_r} & A_\phi &= \left| \frac{\bar{\phi}}{\delta_r} \right| \cos \Phi_{\phi\delta_r} \\ A_\psi &= \left| \frac{\bar{\psi}}{\delta_r} \right| \cos \Phi_{\psi\delta_r} & A_{a_y} &= \left| \frac{\bar{a}_y}{\delta_r} \right| \cos \Phi_{a_y\delta_r} \end{aligned} \right\} \quad (8)$$

$$\left. \begin{aligned} B_\beta &= \left| \frac{\bar{\beta}}{\delta_r} \right| \sin \Phi_{\beta\delta_r} & B_\phi &= \left| \frac{\bar{\phi}}{\delta_r} \right| \sin \Phi_{\phi\delta_r} \\ B_\psi &= \left| \frac{\bar{\psi}}{\delta_r} \right| \sin \Phi_{\psi\delta_r} & B_{a_y} &= \left| \frac{\bar{a}_y}{\delta_r} \right| \sin \Phi_{a_y\delta_r} \end{aligned} \right\} \quad (9)$$

The derivatives of β are represented as

$$\begin{aligned} D\beta &= \omega \left| \frac{\bar{\beta}}{\delta_r} \right| e^{i(\Phi_{\beta\delta_r} + \frac{\pi}{2})} \\ &= \omega \left| \frac{\bar{\beta}}{\delta_r} \right| (-\sin \Phi_{\beta\delta_r} + i \cos \Phi_{\beta\delta_r}) \\ &= -\omega B_\beta + i\omega A_\beta \end{aligned} \quad (10)$$

and

$$\begin{aligned} D^2\beta &= \omega^2 \left| \frac{\bar{\beta}}{\delta_r} \right| e^{i(\Phi_{\beta\delta_r} + \pi)} \\ &= \omega^2 \left| \frac{\bar{\beta}}{\delta_r} \right| (-\cos \Phi_{\beta\delta_r} - i \sin \Phi_{\beta\delta_r}) \\ &= -\omega^2 A_\beta - i\omega^2 B_\beta \end{aligned} \quad (11)$$

Similarly, for roll (see fig. 2(b)), the equations corresponding to equations (7), (10), and (11) would be

$$\phi = A_\phi + iB_\phi \quad (12)$$

$$D\phi = -\omega B_\phi + i\omega A_\phi \quad (13)$$

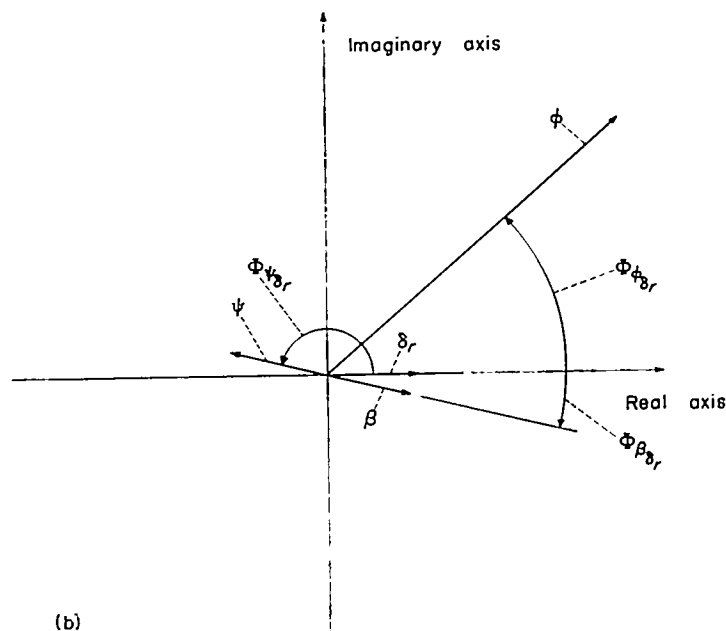
$$D^2\phi = -\omega^2 A_\phi - i\omega^2 B_\phi \quad (14)$$

for yaw,

$$\psi = A_\psi + iB_\psi \quad (15)$$

$$D\psi = -\omega B_\psi + i\omega A_\psi \quad (16)$$

$$D^2\psi = -\omega^2 A_\psi - i\omega^2 B_\psi \quad (17)$$



(b) Vector diagram showing relative magnitudes and positions of input δ_r and response vectors β , ϕ , and ψ .

FIGURE 2.—Concluded.

and, for lateral acceleration,

$$a_y = A_{a_y} + iB_{a_y} \quad (18)$$

Substituting equations (4) to (18) into equations (1), (1a), (2), and (3) and equating the real and imaginary values in each equation yields the following eight simplified equations: From equation (1):

$$K_1 B_\beta - K_2 B_\phi = -\omega (A_\beta + A_\psi) \quad (19)$$

and

$$K_1 A_\beta - K_2 A_\phi = F_1 + \omega (B_\beta + B_\psi) \quad (20)$$

From equation (1a):

$$VK_1 B_\beta = -B_{a_y} \quad (21)$$

$$VK_1 A_\beta = VF_1 - A_{a_y} \quad (22)$$

From equation (2):

$$K_3 B_\beta + K_4 \omega A_\phi + K_5 \omega^2 B_\psi - K_6 \omega A_\psi = \omega^2 B_\phi \quad (23)$$

and

$$K_3 A_\beta - K_4 \omega B_\phi + K_5 \omega^2 A_\psi + K_6 \omega B_\psi - F_2 = \omega^2 A_\phi \quad (24)$$

From equation (3):

$$-K_7 B_\beta + K_8 \omega^2 B_\phi - K_9 \omega A_\psi + K_{10} \omega A_\psi = \omega^2 B_\psi \quad (25)$$

and

$$-K_7 A_\beta + K_8 \omega^2 A_\phi + K_9 \omega B_\psi - K_{10} \omega B_\psi - F_3 = \omega^2 A_\psi \quad (26)$$

In equations (19) to (26) the A_{β,ϕ,ψ,a_y} and B_{β,ϕ,ψ,a_y} terms will be available at the particular values of ω from the frequency-response curves. It will be assumed that the K_2 term is determined from the velocity measurement and the K_5 and K_8 terms, which are equal to the ratios I_{xz}/I_x and I_{xz}/I_z , respectively, are known from either weight and balance calculations or measurements so that only the values of $K_{1,3,4,6,7,9,10}$ and $F_{1,2,3}$ are to be determined from the data. (It should be noted that even though K_5 and K_8 are assumed

to be known a need still exists for a simple method of determining aircraft moments of inertia and the location of the principal longitudinal axis.)

Equations (19) to (26) are now used to compute the K and F coefficients. The advantage of separating each of the equations of lateral motion into real and imaginary equations now becomes apparent. The two derivatives most difficult to determine are C_{lr} and C_{nr} contained in the K_8 and K_9 coefficients, respectively. The K_8 coefficient may be eliminated between equations (23) and (24); similarly the K_9 coefficient may be eliminated between equations (25) and (26). The equations thus obtained, when used to compute the unknown coefficients, result in better conditioned matrices and more accurate results. In the usual case, it has been found unnecessary to perform the elimination of the K_8 coefficient.

As a first step in solving for the K and F coefficients, equations (19) to (26) are fitted to the frequency-response data over a range of values of ω by the method of least squares. The theory of least squares is well known and is

derived in many textbooks (e. g., ref. 9) and no attempt is made here to repeat its derivation.

The application of the least-squares method to equations (19) and (26) converts these equations to their computational form. It is recommended that, if the lateral-acceleration frequency response is available, equations (21) and (22) be used in preference to equations (19) and (20) for the computation of K_1 and F_1 .

Equation (19) may be expressed simply as

$$K_1 = \frac{\sum_{j=\omega_1}^{\omega_n} [K_2 B_\phi - \omega(A_\beta + A_\psi)]_j (B_\beta)_j}{\sum_{j=\omega_1}^{\omega_n} [(B_\beta)_j]^2} \quad (27)$$

and yields K_1 . Similarly, equation (20) can be expressed as

$$F_1 = \frac{1}{n} \sum_{j=\omega_1}^{\omega_n} (K_1 A_\beta - K_2 A_\phi - \omega B_\beta - \omega B_\psi)_j \quad (28)$$

and yields F_1 .

For the same variables K_1 and F_1 , the least-squares forms of equations (21) and (22) for use with the lateral-acceleration frequency response are:

$$K_1 = \frac{\sum_{j=\omega_1}^{\omega_n} (-B_{ay})_j (VB_\beta)_j}{\sum_{j=\omega_1}^{\omega_n} [(VB_\beta)_j]^2} \quad (29)$$

$$F_1 = \frac{1}{n} \sum_{j=\omega_1}^{\omega_n} \left(K_1 A_\beta + \frac{A_{ay}}{V} \right)_j \quad (30)$$

Equation (25) can be expressed as

$$\begin{bmatrix} \sum_{j=\omega_1}^{\omega_n} [(-B_\beta)_j]^2 & \sum_{j=\omega_1}^{\omega_n} (-\omega A_\phi)_j (-B_\beta)_j & \sum_{j=\omega_1}^{\omega_n} (\omega A_\psi)_j (-B_\beta)_j \\ \sum_{j=\omega_1}^{\omega_n} (-B_\beta)_j (-\omega A_\phi)_j & \sum_{j=\omega_1}^{\omega_n} [(-\omega A_\phi)_j]^2 & \sum_{j=\omega_1}^{\omega_n} (\omega A_\psi)_j (-\omega A_\phi)_j \\ \sum_{j=\omega_1}^{\omega_n} (-B_\beta)_j (\omega A_\psi)_j & \sum_{j=\omega_1}^{\omega_n} (-\omega A_\phi)_j (\omega A_\psi)_j & \sum_{j=\omega_1}^{\omega_n} [(\omega A_\psi)_j]^2 \end{bmatrix} \begin{Bmatrix} K_7 \\ K_9 \\ K_{10} \end{Bmatrix} = \begin{Bmatrix} \sum_{j=\omega_1}^{\omega_n} (\omega^2 B_\psi - K_8 \omega^2 B_\phi)_j (-B_\beta)_j \\ \sum_{j=\omega_1}^{\omega_n} (\omega^2 B_\psi - K_8 \omega^2 B_\phi)_j (-\omega A_\phi)_j \\ \sum_{j=\omega_1}^{\omega_n} (\omega^2 B_\psi - K_8 \omega^2 B_\phi)_j (\omega A_\psi)_j \end{Bmatrix} \quad (31)$$

and yields K_7 , K_9 , and K_{10} .

Equation (26) can be expressed as

$$F_3 = \frac{1}{n} \sum_{j=\omega_1}^{\omega_n} (-K_7 A_\beta + K_8 \omega^2 A_\phi + K_9 \omega B_\phi - K_{10} \omega B_\psi - \omega^2 A_\psi)_j \quad (32)$$

and yields F_3 .

In order to evaluate the remaining constants, K_3 , K_4 , K_6 , and F_2 , the coefficient K_8 is first eliminated between equations (23) and (24). This step is taken in order to obtain a more accurate value of the coefficient K_6 , which is less significant under these conditions, and to provide a better conditioned matrix of coefficients in the computation of K_3 , K_4 , and F_2 . Upon elimination of the K_8 term between equations (23) and (24), the following relation is obtained:

$$K_3(B_\beta B_\psi + A_\beta A_\psi) + K_4(\omega A_\phi B_\psi - B_\phi A_\psi) - F_2 A_\psi = \omega^2(B_\phi B_\psi + A_\phi A_\psi) - K_6 \omega^2 \left| \frac{\bar{\psi}}{\delta_r} \right|^2 \quad (33)$$

Upon the application of the method of least squares, equation (33) becomes

$$\left[\begin{array}{ccc} \sum_{j=\omega_1}^{\omega_n} [(B_\beta B_\psi + A_\beta A_\psi)_j]^2 & \sum_{j=\omega_1}^{\omega_n} (\omega A_\phi B_\psi - \omega B_\phi A_\psi)_j (B_\beta B_\psi + A_\beta A_\psi)_j & \sum_{j=\omega_1}^{\omega_n} (-A_\psi)_j (B_\beta B_\psi + A_\beta A_\psi)_j \\ \sum_{j=\omega_1}^{\omega_n} (B_\beta B_\psi + A_\beta A_\psi)_j (\omega A_\phi B_\psi - \omega B_\phi A_\psi)_j & \sum_{j=\omega_1}^{\omega_n} [(\omega A_\phi B_\psi - \omega B_\phi A_\psi)_j]^2 & \sum_{j=\omega_1}^{\omega_n} (-A_\psi)_j (\omega A_\phi B_\psi - \omega B_\phi A_\psi)_j \\ \sum_{j=\omega_1}^{\omega_n} (-A_\psi)_j (B_\beta B_\psi + A_\beta A_\psi)_j & \sum_{j=\omega_1}^{\omega_n} (-A_\psi)_j (\omega A_\phi B_\psi - \omega B_\phi A_\psi)_j & \sum_{j=\omega_1}^{\omega_n} [(-A_\psi)_j]^2 \end{array} \right] \left\{ \begin{array}{c} K_3 \\ K_4 \\ F_2 \end{array} \right\} =$$

$$\left\{ \begin{array}{c} \sum_{j=\omega_1}^{\omega_n} \left(\omega^2 B_\beta B_\psi + \omega^2 A_\phi A_\psi - K_5 \omega^2 \left| \frac{\psi}{\delta_r} \right|^2 \right)_j (B_\beta B_\psi + A_\beta A_\psi)_j \\ \sum_{j=\omega_1}^{\omega_n} \left(\omega^2 B_\phi B_\psi + \omega^2 A_\phi A_\psi - K_5 \omega^2 \left| \frac{\bar{\psi}}{\delta_r} \right|^2 \right)_j (\omega A_\phi B_\psi - \omega B_\phi A_\psi)_j \\ \sum_{j=\omega_1}^{\omega_n} \left(\omega^2 B_\phi B_\psi + \omega^2 A_\phi A_\psi - K_5 \omega^2 \left| \frac{\bar{\psi}}{\delta_r} \right|^2 \right)_j (-A_\psi)_j \end{array} \right\} \quad (34)$$

which yields K_3 , K_4 , and F_2 .

The K_6 coefficient may now be obtained from equation (24) which, after the method of least squares has been applied, may be expressed as:

$$K_6 = \frac{\sum_{j=\omega_1}^{\omega_n} (F_2 + \omega^2 A_\phi - K_5 \omega^2 A_\psi + K_4 \omega B_\phi - K_3 A_\beta)_j (\omega B_\psi)_j}{\sum_{j=\omega_1}^{\omega_n} [(\omega B_\psi)_j]^2} \quad (35)$$

An alternate expression for K_6 may be obtained from equation (23) which may be expressed as

$$K_6 = \frac{\sum_{j=\omega_1}^{\omega_n} (K_3 B_\beta + K_4 \omega A_\phi + K_5 \omega^2 B_\psi - \omega^2 B_\phi)_j (\omega A_\psi)_j}{\sum_{j=\omega_1}^{\omega_n} [(\omega A_\psi)_j]^2} \quad (36)$$

Values of K_6 , which define the derivative C_{l_r} , are important in the spiral mode. In order to obtain accurate values of K_6 , aircraft motions which bring out the full effect of the long-period spiral mode should be analyzed to obtain accurate frequency-response data near $\omega=0$.

In the case where the solution for C_{n_p} is found to involve ill conditioned matrices, K_6 should be eliminated between the real and imaginary equations (25) and (26).

With all the K and F coefficients of the equations of motion determined, the lateral-stability derivatives can be computed from the K and F coefficients and the known aerodynamic parameters by use of the definitions of table I. The transfer-function coefficients can be calculated from the definitions in table II and the transfer functions and modes of lateral motion can be obtained from the equations in appendix A.

SUGGESTED PROCEDURE

In order to aid in the application of this method to the analysis of flight data, a suggested step-by-step procedure which is presented in this section has been worked out. An effort has been made to schedule the procedure so as to reduce the dependence of the results on the derivatives that can be least accurately obtained from the particular data being analyzed. Alternate steps are suggested where it was found that some particular derivative might be more accurately determined by one or the other of two approaches

under certain conditions. No weighting of specific groups of data is employed in the least-squares procedure; however, weighting can be employed when it is considered desirable to put more dependence on data regarded as more reliable.

As a further demonstration of the method, two numerical examples have been carried out according to this procedure. In one example, presented in appendix B, the lateral-stability derivatives are calculated for an airplane whose transient responses to aileron deflection are assumed to be known. This example was chosen in order to gain some insight into the dependence of the method on the accuracy with which the frequency response can be obtained from the transient response.

The other example is for the hypothetical rigid airplane whose mass and geometric parameters are listed in table III. The assumed frequency-response data of sideslip angle β , roll angle ϕ , yaw angle ψ , and lateral acceleration a_y for a rudder-deflection input such as might be obtained from analysis of flight data are listed in table IV and plotted in figures 3 to 6. The analysis of these data has been used to illustrate the following suggested procedure:

(1) Tabulate parameters and working equations

Tabulate the airplane parameters and any stability derivatives that are known or can be computed directly from those that are known as illustrated in table III. Tabulate the least-squares equations (27) to (32) and (34) to (36) with any known terms on the right-hand side as has been done in equations (27a) to (32a) and (34a) to (36a) in table V for the example. (Since C_{n_p} was taken to be zero in the example, all terms containing K_6 were dropped; however, in the example of appendix B, C_{n_p} was included and the K_6 term was determined.)

(2) Tabulate frequency-response data

Tabulate the amplitudes and phase angles of the four lateral variables at the values of ω to be used in the analysis. For simplicity in the example, as shown in table IV, 10 integral values of ω , evenly distributed over the range of the data, were chosen; however, in cases where more accurate points occur at non-integral values of ω , it is advisable to use such points where possible. The range of values of ω should be restricted to the rigid response.

TABLE II.—COEFFICIENTS OF TRANSFER FUNCTIONS

The equations for the transfer functions are given in appendix A; the coefficients C_n are obtained from the coefficients C_n' by dividing by C_0' (e.g., $C_1 = \frac{C_1'}{C_0'}$)

$$\begin{aligned}
 C_0' &= 1 - K_5 K_8 \\
 C_1' &= K_1 + K_4 + K_{10} - K_5 K_9 - K_6 K_8 - K_1 K_5 K_8 \\
 C_2' &= K_7 + K_1 K_4 + K_1 K_{10} + K_4 K_{10} - K_5 K_8 - K_6 K_9 - K_1 K_5 K_9 - K_1 K_6 K_8 \\
 C_3' &= K_2 K_3 + K_4 K_7 - K_5 K_9 + K_1 K_4 K_{10} - K_1 K_6 K_9 - K_2 K_5 K_7 \\
 C_4' &= K_2 K_3 K_{10} - K_2 K_6 K_7 \\
 C_5' &= F_1 (1 - K_5 K_8) \\
 C_6' &= F_1 K_4 + F_1 K_{10} - K_5 F_2 - F_3 - F_1 K_5 K_9 - F_1 K_6 K_8 \\
 C_7' &= F_1 K_4 K_{10} - F_2 K_9 + F_3 K_2 K_5 - F_3 K_4 + F_2 K_2 - F_1 K_6 K_9 \\
 C_8' &= F_3 K_2 K_6 + F_2 K_{10} K_2 \\
 C_9' &= F_2 + F_3 K_5 \\
 C_{10}' &= F_2 K_1 + F_1 K_5 K_7 - F_1 K_3 + F_3 K_6 + F_2 K_1 K_5 + F_2 K_{10} \\
 C_{11}' &= F_2 K_1 K_{10} + F_1 K_6 K_7 + F_2 K_3 + F_2 K_7 - F_1 K_3 K_{10} + F_3 K_1 K_4 \\
 C_{12}' &= F_3 + K_6 F_2 \\
 C_{13}' &= F_3 K_4 + F_3 K_1 - F_1 K_3 K_8 + F_1 K_7 + F_2 K_9 + F_2 K_1 K_5 \\
 C_{14}' &= F_3 K_1 K_4 - F_1 K_3 K_9 + F_1 K_4 K_7 + F_2 K_1 K_9 \\
 C_{15}' &= F_2 K_2 K_7 + F_3 K_2 K_3 \\
 C_{16}' &= C_0' V F_1 \\
 C_{17}' &= C_1' V F_1 - V K_1 C_5' \\
 C_{18}' &= V F_1 C_2' - V K_1 C_6' \\
 C_{19}' &= V F_1 C_3' - V K_1 C_7' \\
 C_{20}' &= V F_1 C_4' - V K_1 C_8'
 \end{aligned}$$

TABLE III.—AIRPLANE PARAMETERS USED IN EXAMPLE GIVEN IN BODY OF REPORT

| (a) Known | |
|--|--|
| $M=0.8$ (evaluated for an altitude of 10,000 ft) | |
| $b=22.6$ ft | |
| $S=130.0$ sq ft | |
| $\rho=0.001756$ slug/cu ft | |
| $V=861.74$ ft/sec | |
| $I_x=2062$ slug-ft ² | |
| $I_z=13,298$ slug-ft ² | |
| $m=\frac{W}{g}=295.03$ slugs | |
| $I_{xz}=157$ slug-ft ² | |
| $C_{n_p}=0$ | |
| (b) Computed | |
| $\tau=\frac{m}{\rho S V}=1.5$ sec | |
| $\mu_b=\frac{m}{\rho S b}=57.2$ | |
| $\bar{C}_L=\frac{W}{q S}=0.1121$ | |
| $K_5=\frac{I_{xz}}{I_x}=0.07614$ | |
| $K_8=\frac{I_{xz}}{I_z}=0.011806$ | |
| $K_2=\frac{g}{V}=0.0374$ per sec | |
| $K_9=C_{n_p}\left[\frac{1}{4\tau(k_z/b)^2}\right]=0$ | |

TABLE IV.—FREQUENCY-RESPONSE DATA FOR EXAMPLE GIVEN IN BODY OF REPORT

| (a) Sideslip, β | | | | |
|--|---------------------------------------|-------------------------------|---|---|
| $\frac{\omega, \text{ radians}}{\text{sec}}$ | $\left \frac{\beta}{\delta_r}\right $ | $\Phi_{\beta_r}, \text{ deg}$ | $A_\beta = \left \frac{\beta}{\delta_r}\right \cos \Phi_{\beta_r}$ | $B_\beta = \left \frac{\beta}{\delta_r}\right \sin \Phi_{\beta_r}$ |
| 1 | 0.536 | -0.1 | 0.536179 | -0.000965 |
| 2 | .574 | -1.1 | .574106 | -.011025 |
| 3 | .650 | -2.3 | .649929 | -.026083 |
| 4 | .797 | -4.1 | .794967 | -.050988 |
| 5 | 1.116 | -8.2 | 1.104368 | -.169106 |
| 6 | 2.105 | -20.8 | 1.967417 | -.747357 |
| 7 | 4.338 | -109.7 | -1.462174 | -4.033763 |
| 8 | 1.368 | -153.1 | -1.268821 | -.510100 |
| 9 | .715 | -163.1 | -.683781 | -.171676 |
| 10 | .484 | -169.1 | -.455533 | -.087720 |

| (b) Roll, ϕ | | | | |
|--|--------------------------------------|------------------------------|--|--|
| $\frac{\omega, \text{ radians}}{\text{sec}}$ | $\left \frac{\phi}{\delta_r}\right $ | $\Phi_{\phi_r}, \text{ deg}$ | $A_\phi = \left \frac{\phi}{\delta_r}\right \cos \Phi_{\phi_r}$ | $B_\phi = \left \frac{\phi}{\delta_r}\right \sin \Phi_{\phi_r}$ |
| 1 | 8.761 | 79.0 | 1.676642 | 8.598903 |
| 2 | 4.624 | 67.7 | 1.754636 | 4.278325 |
| 3 | 3.432 | 57.4 | 1.850166 | 2.891147 |
| 4 | 3.111 | 47.6 | 2.096761 | 2.297675 |
| 5 | 3.459 | 37.1 | 2.760823 | 2.034203 |
| 6 | 5.446 | 18.9 | 5.153317 | 1.762687 |
| 7 | 6.719 | -74.6 | 2.578202 | -9.370572 |
| 8 | 2.729 | -123.9 | -1.638903 | -2.181509 |
| 9 | 1.253 | -138.2 | -.966716 | -.865863 |
| 10 | .780 | -143.9 | -.630341 | -.459096 |

| (c) Yaw, ψ | | | | |
|--|--------------------------------------|------------------------------|--|--|
| $\frac{\omega, \text{ radians}}{\text{sec}}$ | $\left \frac{\psi}{\delta_r}\right $ | $\Phi_{\psi_r}, \text{ deg}$ | $A_\psi = \left \frac{\psi}{\delta_r}\right \cos \Phi_{\psi_r}$ | $B_\psi = \left \frac{\psi}{\delta_r}\right \sin \Phi_{\psi_r}$ |
| 1 | 0.223 | 163.4 | -0.213722 | 0.063714 |
| 2 | .494 | 174.4 | -.491634 | .048463 |
| 3 | .613 | 174.4 | -.610140 | .059934 |
| 4 | .773 | 172.8 | -.767134 | .096775 |
| 5 | 1.096 | 168.9 | -1.075250 | .210567 |
| 6 | 2.079 | 156.2 | -1.903129 | .837405 |
| 7 | 4.299 | 67.3 | 1.656940 | 3.966906 |
| 8 | 1.368 | 18.7 | 1.285597 | .436504 |
| 9 | .710 | 10.7 | .698169 | .131797 |
| 10 | .462 | 7.1 | .458498 | .057029 |

| (d) Lateral acceleration, a_y | | | | |
|--|--|---------------------------|---|---|
| $\frac{\omega, \text{ radians}}{\text{sec}}$ | $\left \frac{a_y}{\delta_r}\right , \frac{\text{ft/sec}^2}{\text{radian}}$ | $\Phi_{a_y}, \text{ deg}$ | $A_{a_y} = \left \frac{a_y}{\delta_r}\right \cos \Phi_{a_y}$ | $B_{a_y} = \left \frac{a_y}{\delta_r}\right \sin \Phi_{a_y}$ |
| 1 | 107.67 | 179.7 | -107.6736 | 0.564215 |
| 2 | 131.70 | 178.2 | -121.6356 | 3.928440 |
| 3 | 149.83 | 178.5 | -149.5411 | 9.277399 |
| 4 | 204.00 | 174.0 | -202.8943 | 21.205800 |
| 5 | 322.10 | 169.6 | -316.7986 | 58.143795 |
| 6 | 691.42 | 156.5 | -634.3160 | 275.150748 |
| 7 | 1628.37 | 67.3 | 627.9656 | 1502.418071 |
| 8 | 587.34 | 18.6 | 556.6625 | 187.337711 |
| 9 | 350.66 | 10.4 | 344.9205 | 63.200245 |
| 10 | 254.54 | 7.2 | 252.5535 | 31.756598 |

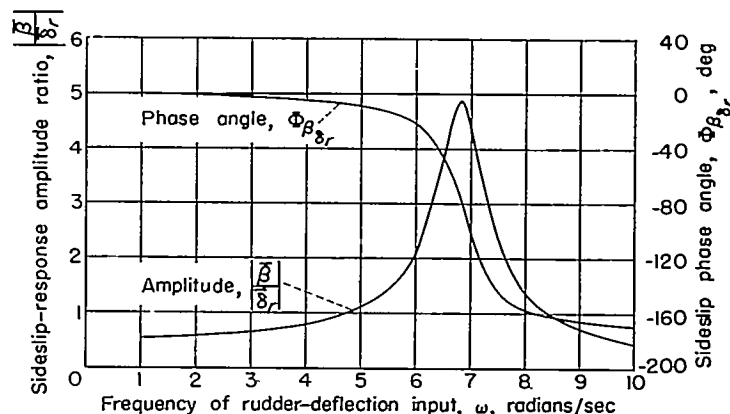


FIGURE 3.—Frequency response in sideslip due to rudder-deflection input for rigid, high-speed airplane of example given in body of report.

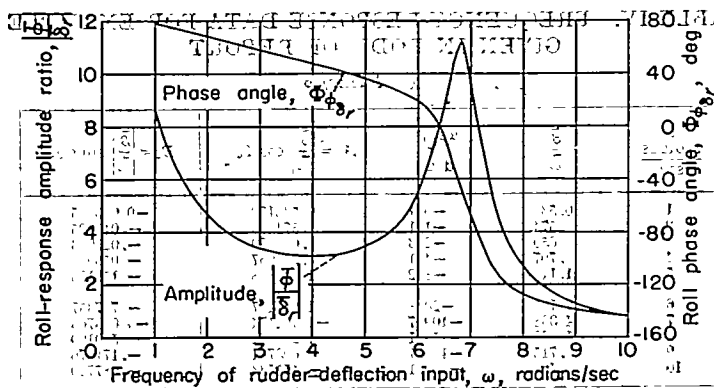


FIGURE 4.—Frequency response in roll due to rudder-deflection input for rigid, high-speed airplane of example given in body of report.

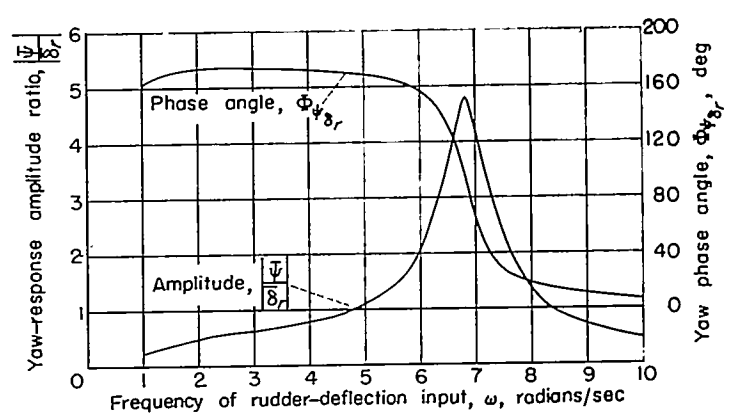


FIGURE 5.—Frequency response in yaw due to rudder-deflection input for rigid, high-speed airplane of example given in body of report.

TABLE V.—MODIFIED FORM OF EQUATIONS USED IN EXAMPLE GIVEN IN BODY OF REPORT

$$\left[\sum_{j=\omega_1}^{\omega_n} [(B_{\delta})_j]^2 \right] \{K_1\} = \left\{ \sum_{j=\omega_1}^{\omega_n} (-\omega A_{\delta} - \omega A_{\psi} + K_2 B_{\delta})_j (B_{\delta})_j \right\} \quad (27a)$$

$$nF_1 = \sum_{j=\omega_1}^{\omega_n} (K_1 A_{\delta} - K_2 A_{\psi} - \omega B_{\delta} - \omega B_{\psi}), \quad (28a)$$

$$\left[\sum_{j=\omega_1}^{\omega_n} [(-VB_{\delta})_j]^2 \right] \{K_1\} = \left\{ \sum_{j=\omega_1}^{\omega_n} (B_{a_{\psi}})_j (-VB_{\delta})_j \right\} \quad (29a)$$

$$nF_2 = \sum_{j=\omega_1}^{\omega_n} \left(K_1 A_{\delta} + \frac{A_{a_{\psi}}}{V} \right), \quad (30a)$$

$$\left[\begin{array}{c} \sum_{j=\omega_1}^{\omega_n} [(-B_{\delta})_j]^2 \\ \sum_{j=\omega_1}^{\omega_n} (-B_{\delta})_j (\omega A_{\psi})_j \\ \sum_{j=\omega_1}^{\omega_n} [(\omega A_{\psi})_j]^2 \end{array} \right] \left\{ \begin{array}{c} K_7 \\ K_{10} \end{array} \right\} = \left\{ \begin{array}{c} \sum_{j=\omega_1}^{\omega_n} (\omega^2 B_{\psi} - K_8 \omega^2 B_{\delta})_j (-B_{\delta})_j \\ \sum_{j=\omega_1}^{\omega_n} (\omega^2 B_{\psi} - K_8 \omega^2 B_{\delta})_j (\omega A_{\psi})_j \end{array} \right\} \quad (31a)$$

$$nF_3 = \sum_{j=\omega_1}^{\omega_n} (-K_7 A_{\delta} + K_8 \omega^2 A_{\psi} - K_{10} \omega B_{\psi} - \omega^2 A_{\psi}), \quad (32a)$$

$$\left[\begin{array}{c} \sum_{j=\omega_1}^{\omega_n} [(B_{\delta} B_{\psi} + A_{\delta} A_{\psi})_j]^2 \\ \sum_{j=\omega_1}^{\omega_n} (B_{\delta} B_{\psi} + A_{\delta} A_{\psi})_j (\omega A_{\psi} B_{\psi} - \omega B_{\delta} A_{\psi})_j \\ \sum_{j=\omega_1}^{\omega_n} (B_{\delta} B_{\psi} + A_{\delta} A_{\psi})_j (-A_{\psi})_j \end{array} \right] \left\{ \begin{array}{c} K_3 \\ K_4 \\ F_2 \end{array} \right\} = \left\{ \begin{array}{c} \sum_{j=\omega_1}^{\omega_n} (\omega A_{\psi} B_{\psi} - \omega B_{\delta} A_{\psi})_j (B_{\delta} B_{\psi} + A_{\delta} A_{\psi})_j \\ \sum_{j=\omega_1}^{\omega_n} [(\omega A_{\psi} B_{\psi} - \omega B_{\delta} A_{\psi})_j]^2 \\ \sum_{j=\omega_1}^{\omega_n} (\omega A_{\psi} B_{\psi} - \omega B_{\delta} A_{\psi})_j (-A_{\psi})_j \end{array} \right\} \quad (34a)$$

$$K_6 = \frac{\sum_{j=\omega_1}^{\omega_n} (F_2 + \omega^2 A_{\psi}^2 - K_5 \omega^2 A_{\psi} + K_4 \omega B_{\psi} - K_3 A_{\delta})_j (\omega B_{\psi})_j}{\sum_{j=\omega_1}^{\omega_n} [(\omega B_{\psi})_j]^2} \quad (35a)$$

$$K_8 = \frac{\sum_{j=\omega_1}^{\omega_n} (K_3 B_{\delta} + K_5 \omega A_{\psi} + K_6 \omega^2 B_{\psi} - \omega^2 B_{\delta})_j (\omega A_{\psi})_j}{\sum_{j=\omega_1}^{\omega_n} [(\omega A_{\psi})_j]^2} \quad (36a)$$

ni noldeh...
troper to zho...
troper to zho...

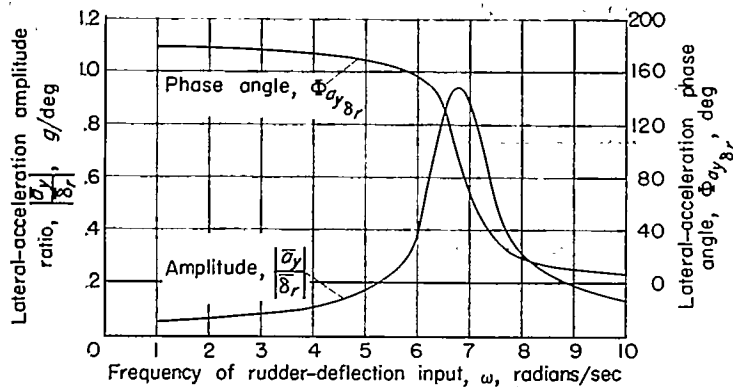


FIGURE 6.—Frequency response in lateral acceleration due to rudder-deflection input for rigid, high-speed airplane of example given in body of report.

(3) Compute vector components of data

Compute the vector components from the data listed in step (2) and tabulate them as shown in table IV. It is advisable to use at least 5-place tables of sine and cosine values in this computation. Additional columns of ωA_β , ωB_β , ωA_ϕ , . . . and $\omega^2 A_\beta$, $\omega^2 B_\beta$, $\omega^2 A_\phi$, . . . will be useful in subsequent operations but are not listed for the example.

(4) Compute K_1

Compute K_1 from equation (27a). (See table VI (a).) In this step and in subsequent steps, summation of the corresponding elements of the indicated products of the data columns evaluates the matrices of coefficients and knowns. The resulting simultaneous equations are readily solved by any standard method.

(4a) Alternate step 4

Compute K_1 from equation (29a). (See table VI (c).)

(5) Compute F_1

Compute F_1 from equation (28a) with the values of K_1 from step (4). (See table VI (b).)

(5a) Alternate step 5

Compute F_1 from equation (30a) with the values of K_1 from step (4a). (See table VI (d).)

(6) Compute K_7 and K_{10}

Compute K_7 and K_{10} from equation (31a). (See table VI (e).)

(7) Compute F_3

Compute F_3 from equation (32a) with the values of K_7 and K_{10} from step (6). (See table VI (f).)

(8) Compute K_3 , K_4 , and F_2

Compute K_3 , K_4 , and F_2 from equation (34a). Because of the combination of two equations to obtain equation (34) in the method, the combination of data columns is more complicated in this step than in others. (See table VI (g).)

(9) Compute K_6

Compute K_6 by one of the following methods:

(a) If F_2 has not been eliminated, calculate K_6 from equation (35a) with the values of K_3 , K_4 , and F_2 from step (8). (See table VI (h).)

(b) If F_2 has been eliminated, calculate K_6 from equation (36a). (See table VI (i).)

(10) Compute stability derivatives

Compute the lateral-stability derivatives from the relationships in table I and the now complete set of values of K and F . (The computed and known values of the K and F coefficients and the stability derivatives for the example are given in tables VII and VIII, respectively.)

(11) Compute transfer-function coefficients
Compute the transfer-function coefficients from the relationships given in table II and the values of K and F . (The computed and known values of the transfer-function coefficients for the example are given in table IX.)

(12) Compute the modes

The modes of lateral motion may now be computed, if desired, by use of the equations in appendix A. (The values of the lateral modes for the example are given in table X).

(13) Accuracy check

When the true derivatives are unknown, the check on the computations is obtained in the following manner: Calculate the frequency response from the equations in appendix A and the computed coefficients of step (11). Compare these values with the data of step (2).

DISCUSSION

DATA REQUIREMENTS

The method of this report is based on the assumption that equations (1), (2), and (3) represent the lateral motions of the airplane. These linear differential equations are satisfied by small variations in roll, yaw, and sideslip but will not necessarily hold for large changes in these variables or in regions of flight where nonlinearities occur. It is therefore desirable to obtain data for transformation to the frequency plane from small motions recorded within ranges of Mach number and other variables in which the coefficients are constant; also, the range of frequency-response data to be used must be limited to values for which the aircraft acts as a rigid body and higher frequency instrument inaccuracies are avoided. Thus, the assumptions of the method will be most nearly in accord with the true physical nature of the problem. In any case, experience has shown that the derivatives obtained by this method of analysis will accurately reproduce the frequency response from which they were extracted.

Since the present method requires flight data in frequency-response form, either the forced-oscillation technique or the technique of oscillating the rudder or aileron at various frequencies and measuring the steady-state response in β , $D\phi$, $D\psi$, and a_r must be employed or the transformation of a transient response from the time plane to the frequency plane must be made by an appropriate method. A comprehensive survey of methods for effecting this transformation from time to frequency plane is given in reference 8 which evaluates the Fourier integral method as well as the use of devices such as the Fourier synthesizer, Coradi harmonic analyzer, and IBM machines for obtaining frequency response from transient-response data.

If, as is usually the case, the transient responses in roll and yaw are measured in the form of time histories of $D\phi$ and $D\psi$ rather than of ϕ and ψ , it is recommended that these time histories of $D\phi$ and $D\psi$ be converted to frequency response initially and then the frequency responses of ϕ and ψ be computed from the frequency responses of $D\phi$ and $D\psi$ by use of the relations:

$$\Phi_{D\phi} = \left| \frac{D\phi}{\delta_r} \right| = \omega \left| \frac{\phi}{\delta_r} \right| \quad \text{and} \quad \Phi_{D\psi} = \left| \frac{D\psi}{\delta_r} \right| = \omega \left| \frac{\psi}{\delta_r} \right|$$

and

$$\Phi_{D\phi} = \Phi_{\phi} + 90^\circ \quad \text{and} \quad \Phi_{D\psi} = \Phi_{\psi} + 90^\circ$$

TABLE VI.—LEAST-SQUARES SOLUTION OF EQUATIONS FOR DATA OF EXAMPLE GIVEN IN BODY OF REPORT

| |
|--|
| (a) K_1 , equation (27a) |
| $\sum_{\omega=1}^{10} (-\omega A_\beta - \omega A_\psi + K_2 B_\psi) B_\beta = 7.378$ $\sum_{\omega=1}^{10} (B_\beta)^2 = 17.562$ $17.562 K_1 = 7.378$ $K_1 = 0.420$ |
| (b) F_1 , equation (28a) |
| $\sum_{\omega=1}^{10} (K_1 A_\beta - K_2 A_\psi - \omega B_\beta - \omega B_\psi) = 1.061$ $10 F_1 = 1.061$ $F_1 = 0.1061$ |
| (c) K_1 from lateral-acceleration data, equation (29a) |
| $\sum_{\omega=1}^{10} (-V B_\beta)^2 = 13,042,324$ $\sum_{\omega=1}^{10} (B_\beta) (-V B_\beta) = 5,567,902$ $13,042,000 K_1 = 5,568,000$ $K_1 = 0.427$ |
| (d) F_1 from lateral-acceleration data, equation (30a) |
| $\sum_{\omega=1}^{10} \left(K_1 A_\beta + \frac{A_\psi}{V} \right) = 1.035059$ $10 F_1 = 1.035$ $F_1 = 0.1035$ |
| (e) K_7 and K_{10} , equation (31a) |
| $\sum_{\omega=1}^{10} (-B_\beta)^2 = 17.562397$ $\sum_{\omega=1}^{10} (-B_\beta) \omega A_\psi = 44.47131$ $\sum_{\omega=1}^{10} (\omega A_\psi)^2 = 473.928987$ $\sum_{\omega=1}^{10} (\omega^2 B_\beta - K_9 \omega^2 B_\psi) (-B_\beta) = 856.325838$ $\sum_{\omega=1}^{10} (\omega^2 B_\beta - K_9 \omega^2 B_\psi) (\omega A_\psi) = 2356.791416$ $K_9 = 0.011806 \quad K_9 = 0$ $17.56 K_7 + 44.47 K_{10} = 856.3$ $44.47 K_7 + 473.93 K_{10} = 2356.8$ $K_7 = 47.443$ $K_{10} = 0.5217$ |
| (f) F_3 , equation (32a) |
| $10 F_3 = \sum_{\omega=1}^{10} (-K_7 A_\beta + K_9 \omega^2 A_\psi - K_{10} \omega \beta_\psi - \omega^2 A_\psi) = -251.87$ $F_3 = -25.187$ |

TABLE VI.—LEAST-SQUARES SOLUTION OF EQUATIONS FOR DATA OF EXAMPLE GIVEN IN BODY OF REPORT—Continued

| |
|---|
| (g) K_2 , K_4 , and F_2 equation (34a) |
| $\sum_{\omega=1}^{10} (B_\beta B_\psi + A_\beta A_\psi)^2 = 371.762380$ $\sum_{\omega=1}^{10} (B_\beta B_\psi + A_\beta A_\psi) (\omega A_\psi B_\beta - \omega B_\psi A_\psi) = -3617.677695$ $\sum_{\omega=1}^{10} (B_\beta B_\psi + A_\beta A_\psi) (-A_\psi) = 23.184790$ $\sum_{\omega=1}^{10} (\omega A_\psi B_\beta - \omega B_\psi A_\psi)^2 = 35234.438878$ $\sum_{\omega=1}^{10} (\omega A_\psi B_\beta - \omega B_\psi A_\psi) (-A_\psi) = -209.219323$ $\sum_{\omega=1}^{10} (-A_\psi)^2 = 11.122853$ $\sum_{\omega=1}^{10} \left(\omega^2 B_\beta B_\psi + \omega^2 A_\beta A_\psi - K_2 \omega^2 \left \frac{\psi}{\delta} \right ^2 \right) (B_\beta B_\psi + A_\beta A_\psi) = 33187.734500$ $\sum_{\omega=1}^{10} \left(\omega^2 B_\beta B_\psi + \omega^2 A_\beta A_\psi - K_2 \omega^2 \left \frac{\psi}{\delta} \right ^2 \right) (\omega A_\psi B_\beta - \omega B_\psi A_\psi) = -322344.219155$ $\sum_{\omega=1}^{10} \left(\omega^2 B_\beta B_\psi + \omega^2 A_\beta A_\psi - K_2 \omega^2 \left \frac{\psi}{\delta} \right ^2 \right) (-A_\psi) = 2422.633022$ $371.76238 K_2 - 3617.67769 K_4 + 23.18479 F_2 = 33187.73451$ $-3617.67769 K_2 + 35234.43888 K_4 - 209.21932 F_2 = -322344.21915$ $23.18479 K_2 - 209.21932 K_4 + 11.12285 F_2 = 2422.633022$ $K_2 = 138.272 \quad K_4 = 5.212 \quad F_2 = 27.636$ |
| (h) K_6 , equation (35a) |
| $\sum_{\omega=1}^{10} (\omega B_\psi)^2 = 811.55627$ $\sum_{\omega=1}^{10} (\omega B_\psi) (F_2 + \omega^2 A_\psi - K_5 \omega^2 A_\psi + K_4 \omega B_\psi - K_3 A_\beta) = 235.117592$ $811.6 K_6 = 235.1$ $K_6 = 0.290$ |
| (i) Alternate means of obtaining K_6 , equation (36a) |
| $\sum_{\omega=1}^{10} (\omega A_\psi)^2 = 473.928983$ $\sum_{\omega=1}^{10} (K_2 B_\beta + K_4 \omega A_\psi + K_5 \omega^2 B_\psi - \omega^2 B_\beta) (\omega A_\psi) = 137.774056$ $473.9 K_6 = 137.77$ $K_6 = 0.291$ |

TABLE VII.—COMPARISON OF COMPUTED AND KNOWN VALUES OF COEFFICIENTS OF EQUATIONS OF LATERAL MOTION FOR EXAMPLE GIVEN IN BODY OF REPORT

| Coefficient | Computed from data | Known value |
|-------------|---|--|
| K_1 | $\begin{cases} 0.42054 \\ 0.4269 \end{cases}$ | $\begin{cases} 0.427 \\ 0.427 \end{cases}$ |
| K_2 | 138.272145 | 138.245 |
| K_4 | 5.212593 | 5.21 |
| K_6 | 0.290 | 0.3017 |
| K_7 | 47.438625 | 47.41 |
| K_{10} | 0.521457 | 0.5272 |
| F_1 | $\begin{cases} 0.10609 \\ 0.1035 \end{cases}$ | $\begin{cases} 0.104 \\ 0.104 \end{cases}$ |
| F_2 | 27.636187 | 27.65 |
| F_3 | -25.187091 | -25.22 |

*From sideslip data.

*From lateral-acceleration data.

TABLE VIII.—COMPARISON OF COMPUTED AND KNOWN STABILITY DERIVATIVES FOR EXAMPLE GIVEN IN BODY OF REPORT

| Stability derivative | Computed | Known |
|----------------------|----------|--------|
| $C_{Y\beta}$ | -1.259 | -1.28 |
| $C_{l\beta}$ | -0.1490 | -0.149 |
| $C_{l\dot{\beta}}$ | -0.4280 | -0.428 |
| C_{lr} | 0.02389 | 0.0248 |
| $C_{n\beta}$ | 0.3292 | 0.329 |
| C_{nr} | -0.2732 | -0.279 |
| $C_{r\dot{\beta}}$ | 0.3183 | 0.312 |
| $C_{l\dot{r}}$ | 0.02979 | 0.0298 |
| $C_{n\dot{r}}$ | -0.1748 | -0.175 |

TABLE IX.—COMPARISON OF COMPUTED AND KNOWN COEFFICIENTS OF TRANSFER FUNCTIONS FOR EXAMPLE GIVEN IN BODY OF REPORT

| Coefficient | Computed from data (least-squares value) | Known |
|--------------------------|--|---------------|
| $C_{\delta'}$ | 0.999101 | 0.999101 |
| $C_{\dot{\delta}'}$ | 4.180763 | 4.180264 |
| $C_{\ddot{\delta}'}$ | 50.934290 | 50.972856 |
| $C_{\delta''}$ | 253.483381 | 253.2143 |
| $C_{\dot{\delta}''}$ | 2.193801 | 2.190881 |
| $C_{\delta'''}^*$ | 0.105995 | 0.103907 |
| $C_{\dot{\delta}'''}^*$ | 25.468778 | 25.468886 |
| $C_{\ddot{\delta}'''}^*$ | 132.544801 | 132.64416 |
| $C_{\delta''''}^*$ | 0.267223 | 0.260611 |
| $C_{\dot{\delta}''''}^*$ | 25.718442 | 25.729749 |
| $C_{10'}$ | 3.636361 | 3.952748 |
| $C_{11'}$ | -2174.851610 | -2178.769199 |
| $C_{12'}$ | -24.860818 | -24.863564 |
| $C_{13'}$ | -136.884812 | -137.264852 |
| $C_{14'}$ | -28.978823 | -30.417543 |
| $C_{15'}$ | -81.654072 | -81.36940 |
| $C_{16'}$ | 89.111765 | 89.62096 |
| $C_{17'}$ | 509.187683 | 514.350717 |
| $C_{18'}$ | -4822.026985 | -4815.419163 |
| $C_{19'}$ | -20127.620554 | -20138.324577 |
| $C_{20'}$ | 97.287337 | 100.642037 |

TABLE X.—COMPUTED LATERAL MODES FOR EXAMPLE GIVEN IN BODY OF REPORT

[Characteristic equation is equation (A16) of appendix A]

| | |
|---|-----------------------|
| Damping-in-roll mode, λ_1 ----- | -5.393 |
| Spiral mode, λ_2 ----- | -0.008668 |
| Dutch roll mode, $-\xi \pm i\eta$ ----- | -0.381 $\pm i$ (6.84) |

Flight data are usually measured about the body axes; before they can be used, however, either they must be converted to a form corresponding to the stability axes or the development must be restated in terms of body axes. The following equations are presented to be used in transforming to the stability axes:

$$\phi = \phi_b \cos \alpha + \psi_b \sin \alpha$$

$$\dot{\psi} = \dot{\psi}_b \cos \alpha - \dot{\phi}_b \sin \alpha$$

where α is the angle of attack (angle between the body X -axis and the stability X -axis) and the subscript b refers to the body axes. In addition, the sideslip-vane measurements can be converted to the corresponding values at the center of gravity by means of the formula

$$\beta = \left(\beta_v - \frac{l_{\beta} \dot{\psi}}{V} \right) \cos \alpha$$

where the subscript v refers to the vane and l_{β} is the distance from the center of gravity to the sideslip vane measured along the body X -axis.

If the lateral acceleration a_y as recorded by an accelerometer is used, it must be corrected for any components of angular velocity and acceleration present in such records because of the displacement of the accelerometer from the airplane center of gravity.

SENSITIVITY OF THE METHOD AND POSSIBLE SIMPLIFICATIONS

Even though the foregoing general rules are observed, the question arises as to how the derivatives obtained compare with the actual derivatives of the airplane and how sensitive these derivatives are to inaccuracies in the frequency-response data. These inaccuracies stem from several sources such as measurement of the transient motions, transformation from time to frequency plane, and reading errors. Care should be exercised to keep these inaccuracies to a minimum.

No attempt is made to present a comprehensive error analysis in this report, but several general remarks appear to be in order. A comparison of the values given in tables VII, VIII, and IX for the coefficients of the equations of lateral motion, the lateral-stability derivatives, and the transfer-function coefficients indicates essentially no errors due to the method itself. It has been found, however, that the derived values of $C_{Y\beta}$ and $C_{Y\dot{\beta}}$ are sensitive to slight variations in the quantities A_{β} , B_{β} , $A_{\dot{\beta}}$, and $B_{\dot{\beta}}$ (see eqs. (27) and (28)). This sensitivity is due to the fact that the airplane angle of yaw is very nearly equal to the negative of the sideslip angle and hence accurate determination of the lateral acceleration from measurements of $\dot{\psi}$ and $\dot{\beta}$ is difficult. This difficulty can be obviated by a direct measurement of the lateral acceleration with an accelerometer and more accurate values determined for $C_{Y\beta}$ and $C_{Y\dot{\beta}}$ by means of equations (29) and (30).

As brought out in appendix B, the accuracy with which the values of the derivatives C_{lr} , C_{nr} , and $C_{Y\beta}$ can be determined from frequency-response data appears to be dependent upon the inclusion of data for frequencies near the natural frequency of the airplane. This fact is brought out further by some unpublished results that indicate that derivatives such as C_{nr} and $C_{Y\beta}$ are very sensitive to variations of the frequency responses near the airplane natural frequency. In the case of C_{nr} , the conclusion is obvious since this derivative is known to contribute largely to the airplane Dutch roll damping and it is also known that the peak value of the frequency-response amplitude ratio, say $\left| \frac{\beta}{\delta} \right|$, is highly dependent upon the airplane Dutch roll damping. It appears therefore that an accurate representation of the frequency responses at frequencies near the airplane natural frequency (for instance ± 50 percent) is probably very important in the determination of the lateral-stability derivatives.

In general, when the number of unknown derivatives can be reduced, the remaining derivatives can be determined with greater reliability. For this reason, several possible simplifications are presented for the calculation of the derivatives $C_{n\beta}$, $C_{n\dot{\beta}}$, $C_{l\beta}$, and $C_{l\dot{\beta}}$. The airplane natural

frequency is, for small values of the product of inertia, well approximated by the expression

$$\omega_N^2 \approx C_{n_\beta} \frac{qSb}{I_z}$$

If the natural frequency ω_N is apparent from the available transients and the inertia parameter is known, a very good value of C_{n_β} can generally be obtained from this expression.

Extrapolation of the amplitude ratio $\left| \frac{\beta}{\delta_r} \right|$ to zero frequency may afford a means of obtaining the derivative $C_{n_{\delta_r}}$ subsequent to determination of C_{n_β} from the preceding frequency relation. The value of $\left| \frac{\beta}{\delta_r} \right|$ at $\omega=0$ obtained by this extrapolation is not indicative of the actual static sensitivity, but rather of the apparent static sensitivity which includes the very lightly damped spiral mode. This apparent steady-state response is approximately equal to the ratio $\frac{C_{n_{\delta_r}}}{C_{n_\beta}}$ from which $C_{n_{\delta_r}}$ can be estimated if C_{n_β} is known.

The actual static values of some of the lateral variables may be found theoretically by taking the ratio of the integrals of the time histories of the output and input; for example,

$$\left| \frac{\beta}{\delta_r} \right|_{\omega=0} = \frac{\int_0^\infty \beta dt}{\int_0^\infty \delta_r dt}$$

Probably in certain cases these integrals could be evaluated accurately enough to yield a good approximation to the actual static sensitivities. Some of the stability derivatives influence greatly the values of the transfer functions for $\omega=0$, and use of accurate zero frequency data would undoubtedly lead to better estimates of these stability derivatives.

The transfer function which relates the rolling velocity to aileron deflection is well approximated (particularly at low frequencies) by the expression

$$\frac{\dot{\phi}}{\delta_a}(i\omega) \approx \frac{G_2}{K_4 + i\omega} = \frac{G_2}{(K_4^2 + \omega^2)^{1/2}} e^{-i \tan^{-1} \frac{\omega}{K_4}}$$

Therefore, $\Phi_{\dot{\phi}_{\delta_a}}(\omega) = -\tan^{-1} \frac{\omega}{K_4}$ from which K_4 , and subsequently C_{l_p} , can be determined. Also, by extrapolating the

amplitude ratio $\left| \frac{\dot{\phi}}{\delta_a} \right|$ to $\omega=0$, the parameter G_2 , and hence $C_{l_{\delta_a}}$, can be obtained once K_4 has been determined. As was the case for $\left| \frac{\beta}{\delta_r} \right|$, this extrapolation does not yield the true value of $\left| \frac{\dot{\phi}}{\delta_a} \right|$ at $\omega=0$, which is actually zero, but gives the apparent value due to the lightly damped spiral mode.

CONCLUDING REMARKS

A method has been presented for extracting lateral-stability derivatives from frequency-response data which have been derived from aircraft transient responses to arbitrary control inputs. In order to demonstrate the use of the method, the lateral-stability derivatives have been calculated for two hypothetical airplanes for which the frequency-response data or transient-response flight data were assumed to be known. Simplifications were proposed for obtaining certain of the derivatives, and although no error analysis is presented in this report, some general observations can be made concerning the sensitivity of the method to inaccuracies in the original data.

In view of the limited experience in the determination of lateral-stability derivatives from flight data, and particularly in using the present method, it appears that an investigation should be made to determine the effects of some of the errors inherent in analyses of transient responses, such as recording accuracy, reading accuracy, and so forth, on the derived frequency responses and hence on the computed lateral-stability derivatives. It is noted here that, although the methods presented in this report for the extraction of lateral-stability derivatives from frequency-response data are theoretically correct and mathematically sound, the accuracy with which the lateral-stability derivatives of an airplane can be determined by this method is directly dependent upon the accuracy with which the frequency responses of the airplane are known. Also, some consideration should be given to the types of inputs likely to afford good frequency-response data and to testing procedures whereby some of the stability derivatives that are most difficult to determine may be accurately obtained. In addition, accurate frequency-response data for specific ranges of frequency may yield more accurately certain of the stability derivatives and this possibility should be investigated.

LANGLEY AERONAUTICAL LABORATORY,
NATIONAL ADVISORY COMMITTEE FOR AERONAUTICS,
LANGLEY FIELD, VA., February 16, 1954.

APPENDIX A

DEVELOPMENT OF EQUATIONS FOR TRANSFER FUNCTIONS, MODES, AND FREQUENCY RESPONSE FOR LATERAL MOTION

In this appendix the transfer functions are derived from the equations of lateral motion and the modes and frequency response are expressed in terms of the transfer-function coefficients.

EQUATIONS OF MOTION

The motions of a rigid aircraft resulting from a rudder-deflection input are assumed to be expressed by the following three standard linearized equations of lateral motion:

$$(D+K_1)\beta-K_2\phi+D\psi=F_1\delta_r(t) \quad (A1)$$

$$K_3\beta+(D^2+K_4D)\phi-(K_5D^2+K_6D)\psi=F_2\delta_r(t) \quad (A2)$$

$$-K_7\beta-(K_8D^2+K_9D)\phi+(D^2+K_{10}D)\psi=F_3\delta_r(t) \quad (A3)$$

where the K and F coefficients are defined in table I. The axes and the sign conventions employed are shown in figure 1. On applying the Laplace transformation

$$F(s)=\int_0^\infty f(t)e^{-st}dt \quad (A4)$$

(where $s=\sigma+i\omega$) to both sides of equations (A1), (A2), and (A3) and assuming the initial conditions to be zero, there is obtained

$$\begin{bmatrix} s+K_1 & -K_2 & s \\ K_3 & s^2+K_4s & -K_5s^2-K_6s \\ -K_7 & -K_8s^2-K_9s & s^2+K_{10}s \end{bmatrix} \begin{Bmatrix} \beta(s) \\ \phi(s) \\ \psi(s) \end{Bmatrix} = \begin{Bmatrix} F_1\delta_r(s) \\ F_2\delta_r(s) \\ F_3\delta_r(s) \end{Bmatrix} \quad (A5)$$

$$\begin{bmatrix} s+K_1 & -K_2 & s \\ K_3 & s^2+K_4s & -K_5s^2-K_6s \\ -K_7 & -K_8s^2-K_9s & s^2+K_{10}s \end{bmatrix} \begin{Bmatrix} \beta(s) \\ \phi(s) \\ \psi(s) \end{Bmatrix} = \begin{Bmatrix} F_1\delta_r(s) \\ F_2\delta_r(s) \\ F_3\delta_r(s) \end{Bmatrix} \quad (A6)$$

$$\begin{bmatrix} s+K_1 & -K_2 & s \\ K_3 & s^2+K_4s & -K_5s^2-K_6s \\ -K_7 & -K_8s^2-K_9s & s^2+K_{10}s \end{bmatrix} \begin{Bmatrix} \beta(s) \\ \phi(s) \\ \psi(s) \end{Bmatrix} = \begin{Bmatrix} F_1\delta_r(s) \\ F_2\delta_r(s) \\ F_3\delta_r(s) \end{Bmatrix} \quad (A7)$$

TRANSFER FUNCTIONS

By solving the three simultaneous equations (A5), (A6), and (A7) for $\beta(s)$ there is obtained

$$\begin{aligned} & (C_0's^6+C_1's^4+C_2's^3+C_3's^2+C_4's)\beta(s) \\ & = (C_6's^4+C_6's^3+C_7's^2+C_8's)\delta_r(s) \end{aligned} \quad (A8)$$

where the C_n' coefficients are defined in table II. Dividing equation (A8) through by C_0' and using the unprimed coefficients C_n to designate the ratio of the primed coefficient to C_0' (e. g., $C_1=\frac{C_1'}{C_0'}$ and $C_2=\frac{C_2'}{C_0'}$) results in the following transfer function for β due to a rudder-deflection input δ_r :

$$\frac{\beta}{\delta_r} = \frac{C_6s^4+C_6s^3+C_7s^2+C_8s}{s^4+C_1s^3+C_2s^2+C_3s+C_4} \quad (A9)$$

Determined in a similar manner, the transfer function for ϕ is

$$\frac{\phi}{\delta_r} = \frac{C_9s^2+C_{10}s+C_{11}}{s^4+C_1s^3+C_2s^2+C_3s+C_4} \quad (A10)$$

and the transfer function for ψ is

$$\frac{\psi}{\delta_r} = \frac{C_{12}s^3+C_{13}s^2+C_{14}s+C_{15}}{s^4+C_1s^3+C_2s^2+C_3s+C_4} \quad (A11)$$

The lateral-acceleration transfer function may be developed from the sideslip transfer function in the following manner: The lateral acceleration is usually defined as

$$a_y = V(D\beta+D\psi-K_2\phi) \quad (A12)$$

Substituting equation (A1) into (A12) yields

$$a_y = VF_1\delta_r(t) - VK_1\beta \quad (A13)$$

Therefore,

$$\frac{a_y}{\delta_r} = VF_1 - \frac{\beta(s)}{\delta_r(s)} VK_1 \quad (A14)$$

or

$$\frac{a_y}{\delta_r} = \frac{C_{16}s^4+C_{17}s^3+C_{18}s^2+C_{19}s+C_{20}}{s^4+C_1s^3+C_2s^2+C_3s+C_4} \quad (A15)$$

MODES

The characteristic equation of lateral motion is obtained by expanding the determinant of the coefficients of equations (A1), (A2), and (A3) and is

$$s(s^4+C_1s^3+C_2s^2+C_3s+C_4)=0 \quad (A16)$$

This equation can be factored as follows:

$$s(s+\lambda_1)(s+\lambda_2)(s+\xi-i\eta)(s+\xi+i\eta)=0 \quad (A17)$$

where the root $s=0$ indicates that the aircraft is insensitive to azimuth, the root λ_1 is the damping-in-roll mode, the root λ_2 is the spiral mode, and the root $-\xi\pm i\eta$ is the Dutch roll mode, an oscillatory motion composed of roll, yaw, and sideslip. The modes of this airplane are indicated in table X. An approximate expression for λ_2 which gives excellent results is

$$\lambda_2 = \frac{C_4}{C_3} = \frac{C_4'}{C_3'} \quad (A18)$$

FREQUENCY RESPONSE

The frequency response which is the steady-state response to a sinusoidal input consists of an amplitude-ratio and phase-angle relation between input and response for various values of ω . It is determined by substituting $s=i\omega$ into equations (A9), (A10), (A11), and (A15), respectively, for β , ϕ , ψ , and a_y and is a complex expression. The amplitude ratio is the square root of the sum of the squares of the real and imaginary parts of the complex expression and the phase angle Φ is the arc tangent of the ratio of the imaginary part to the real part.

The amplitude ratio for sideslip angle β is

$$\left| \frac{\beta}{\delta_r} \right| = \sqrt{\frac{(C_6-C_6\omega^2)^2+(C_7\omega-C_8\omega^3)^2}{(\omega^4-C_1\omega^2+C_4)^2+(C_2\omega-C_3\omega^3)^2}} \quad (A19)$$

and the phase-angle relation between β and δ_r is

$$\Phi_{\beta\delta_r} = \tan^{-1} \left(\frac{C_7\omega-C_8\omega^3}{C_6-C_6\omega^2} \right) - \tan^{-1} \left(\frac{C_2\omega-C_3\omega^3}{\omega^4-C_1\omega^2+C_4} \right) \quad (A20)$$

The amplitude ratio for roll ϕ is

$$\left| \frac{\bar{\phi}}{\bar{\delta}_r} \right| = \sqrt{\frac{(C_{11} - C_9 \omega^2)^2 + (C_{10} \omega)^2}{(\omega^4 - C_2 \omega^2 + C_4)^2 + (C_3 \omega - C_1 \omega^3)^2}} \quad (\text{A21})$$

and the phase-angle relation between ϕ and δ_r is

$$\Phi_{\phi, \delta_r} = \tan^{-1} \left(\frac{C_{10} \omega}{C_{11} - C_9 \omega^2} \right) - \tan^{-1} \left(\frac{C_3 \omega - C_1 \omega^3}{\omega^4 - C_2 \omega^2 + C_4} \right) \quad (\text{A22})$$

The amplitude ratio for yaw ψ is

$$\left| \frac{\bar{\psi}}{\bar{\delta}_r} \right| = \sqrt{\frac{(C_{15} - C_{13} \omega^2)^2 + (C_{14} \omega - C_{12} \omega^3)^2}{(C_1 \omega^4 - C_3 \omega^2)^2 + (\omega^5 - C_2 \omega^3 + C_4 \omega)^2}} \quad (\text{A23})$$

and the phase-angle relation between ψ and δ_r is

$$\Phi_{\psi, \delta_r} = \tan^{-1} \left(\frac{C_{14} \omega - C_{12} \omega^3}{C_{15} - C_{13} \omega^2} \right) - \tan^{-1} \left(\frac{\omega^5 - C_2 \omega^3 + C_4 \omega}{C_1 \omega^4 - C_3 \omega^2} \right) \quad (\text{A24})$$

The amplitude ratio for lateral acceleration a_y is

$$\left| \frac{\bar{a}_y}{\bar{\delta}_r} \right| = \sqrt{\frac{(C_{16} \omega^4 - C_{18} \omega^2 + C_{20})^2 + (C_{19} \omega - C_{17} \omega^3)^2}{(\omega^4 - C_2 \omega^2 + C_4)^2 + (C_3 \omega - C_1 \omega^3)^2}} \quad (\text{A25})$$

and the phase-angle relation between a_y and δ_r is

$$\Phi_{a_y, \delta_r} = \tan^{-1} \left(\frac{C_{19} \omega - C_{17} \omega^3}{C_{16} \omega^4 - C_{18} \omega^2 + C_{20}} \right) - \tan^{-1} \left(\frac{C_3 \omega - C_1 \omega^3}{\omega^4 - C_2 \omega^2 + C_4} \right) \quad (\text{A26})$$

APPENDIX B

DETERMINATION OF LATERAL-STABILITY DERIVATIVES BY USE OF FREQUENCY RESPONSES DERIVED FROM CALCULATED TRANSIENT RESPONSES TO AILERON DEFLECTION

Transient responses in roll, yaw, and sideslip to a square-pulse aileron deflection were calculated for the airplane whose mass and aerodynamic characteristics are given in table XI. These transients and assumed aileron time histories are presented in figure 7.

TABLE XI.—PARAMETERS OF AIRPLANE USED AS EXAMPLE IN APPENDIX B

| | |
|--|---------|
| Altitude, ft..... | 30,000 |
| Wing loading, lb/sq ft..... | 65 |
| V, ft/sec..... | 797 |
| b, ft..... | 28 |
| C_L | 0.23 |
| μ_b | 80.7 |
| $K_{\dot{x}^2}$ | 0.0097 |
| $K_{\dot{z}^2}$ | 0.0513 |
| K_{xz} | 0.00145 |
| C_{l_p} per radian..... | -0.40 |
| C_{l_r} per radian..... | 0.08 |
| $C_{l_{\dot{\delta}_a}}$ per radian..... | -0.02 |
| C_{n_r} per radian..... | -0.40 |
| $C_{n_{\dot{\delta}_a}}$ per radian..... | -1.0 |
| $C_{\dot{\delta}_a}$ per radian..... | 0.25 |
| $C_{\dot{\delta}_\beta}$ per radian..... | -0.126 |
| $C_{\dot{\delta}_\beta}$ per radian..... | -0.11 |

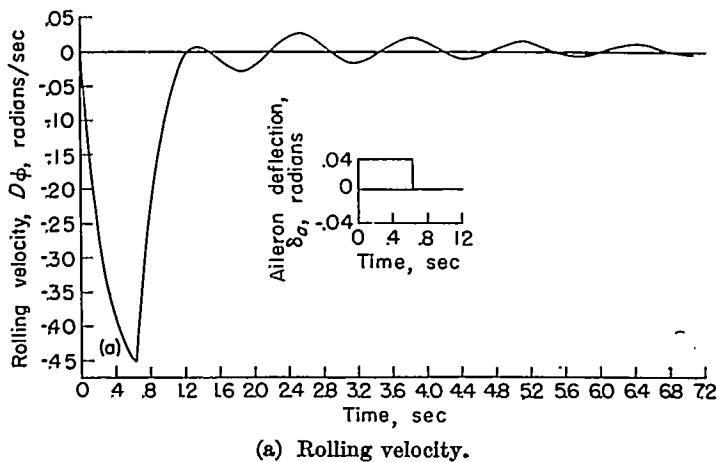


FIGURE 7.—Calculation of transient responses to a square-pulse aileron deflection for the airplane defined in table XI.

The frequency responses $D\phi/\delta_a$, $D\psi/\delta_a$, and β/δ_a were obtained from analysis of the calculated transient responses $D\phi$, $D\psi$, and β to the assumed aileron deflection by use of the equation

$$\frac{\int_0^\infty e^{-st} F(t) dt}{\int_0^\infty e^{-st} q(t) dt} = G(s)$$

The Laplace transforms of the responses were obtained by fitting various functions, such as polynomials or trigonometric functions, to finite sections of the respective output

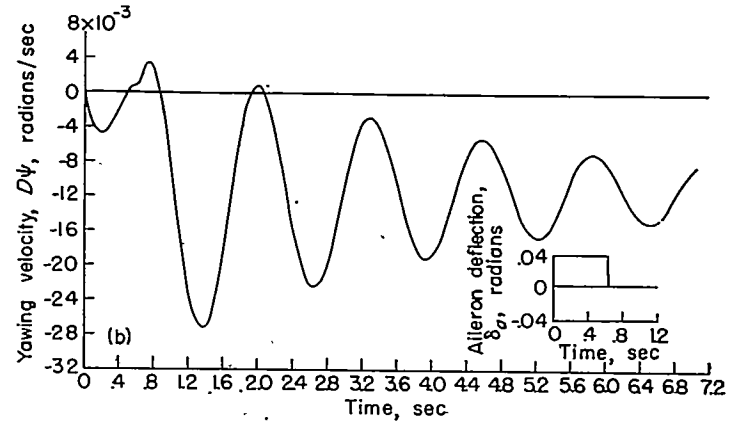


FIGURE 7.—Continued.

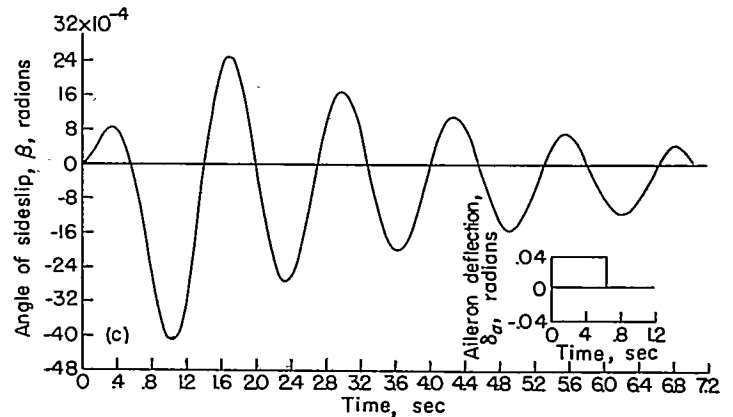


FIGURE 7.—Concluded.

curves and thus performing analytically the required integrations from 0 to ∞ in finite time intervals as described in reference 8. These transforms were then evaluated for a number of values of $i\omega$ (where $s=i\omega$) and frequency-response data were obtained. These data have been plotted in figure 8 where they are represented by the triangular test points.

For purposes of comparison, the frequency responses for the airplane were calculated from the basic mass and aerodynamic characteristics and are also presented in figure 8 in the form of curves. The agreement between these two sets of data is seen to be excellent.

In addition, the frequency responses were obtained from the calculated transients by use of IBM equipment. The Fourier transform of each transient was obtained from a numerical evaluation, by means of the IBM equipment, of the integral

$$\int e^{-i\omega t} F(t) dt$$

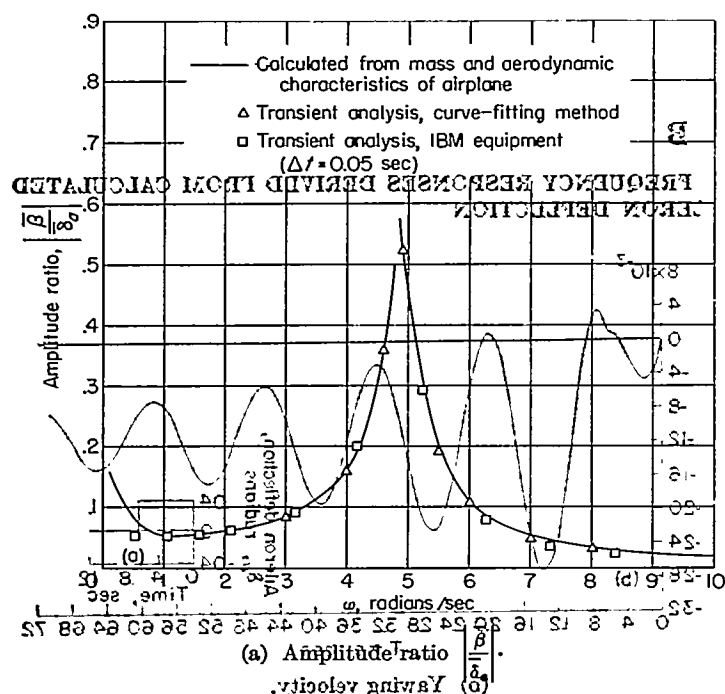
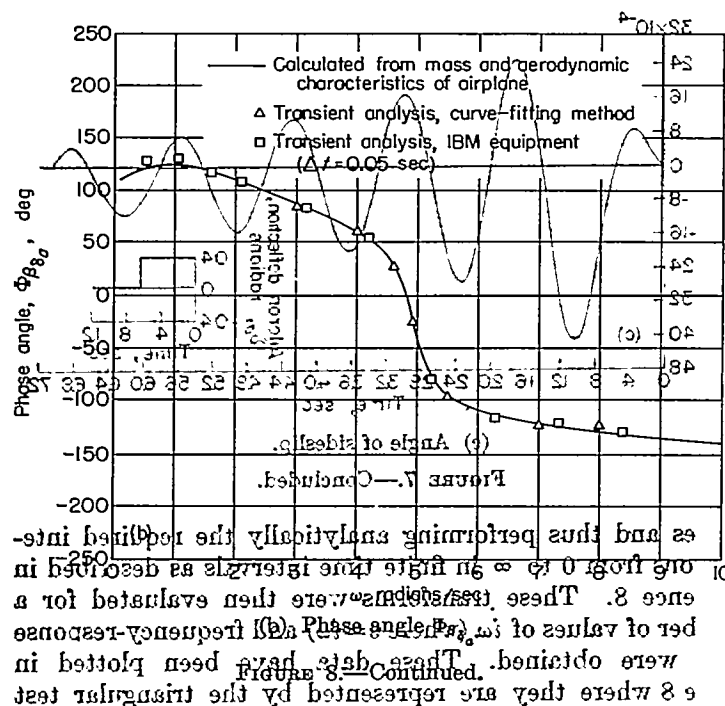


FIGURE 8.—Frequency responses due to aileron-deflection input for the airplane described in table XI.



between the limits of $t=0$ and $t=6.9$ seconds to which was added a correction based on an analytical expression of the transients from $t=6.9$ seconds to infinity. A time interval $\Delta t=0.05$ seconds was used in the numerical integrations. The frequency responses thus obtained are shown in figure 8 as square points and appear to be in excellent agreement with the frequency responses calculated from the basic mass and aerodynamic characteristics and with those derived from the transients by the curve-fitting method. By use of equations (27), (31), (33), (35), and (36) of the body of the report and the frequency-response data derived from the transients by both methods, the coefficients K_1 , K_2 , K_3 , K_4 , K_5 , G_2 , K_7 , K_8 , and K_{10} were obtained, and hence the

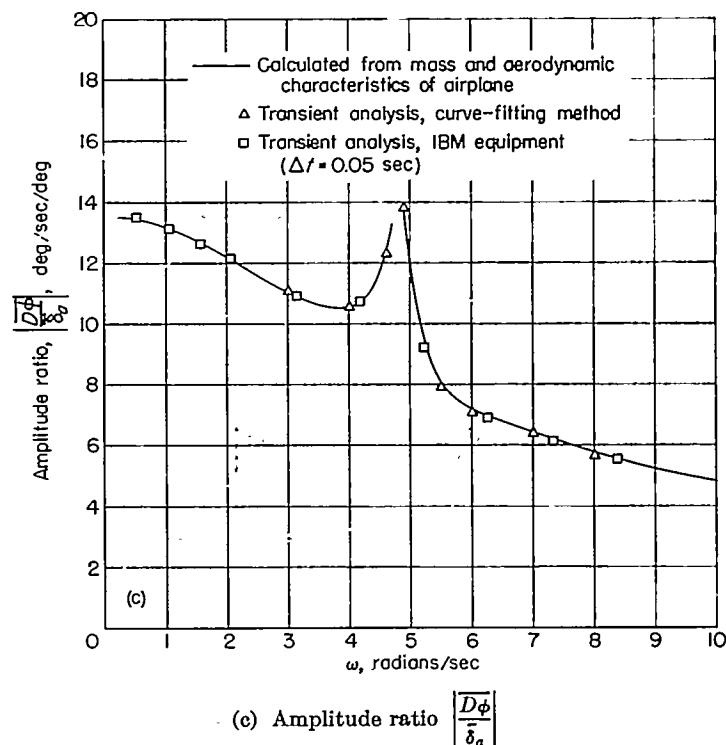


FIGURE 8.—Continued.

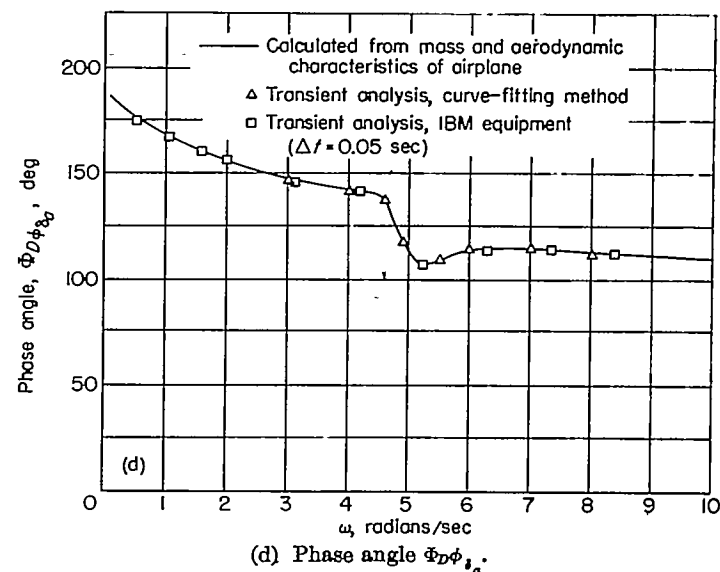


FIGURE 8.—Continued.

stability derivatives C_{r_p} , C_{i_p} , C_{l_p} , C_{l_r} , $C_{l_{\dot{\alpha}}}$, C_{n_p} , C_{n_r} , and $C_{n_{\dot{\alpha}}}$. These results are presented in table XII along with the values assumed for the calculation of the transient motions. Results are also presented for the case where equations (1), (2), and (3) of the body of the report were not separated into real and imaginary parts but were treated as vector equations and the method of least squares applied in a manner similar to that described in reference 4. The amount of work required in the least-squares process as shown in appendix C is less when these equations are treated as vector equations, but a limitation is introduced in that a parameter such as K_8 which is difficult to extract with

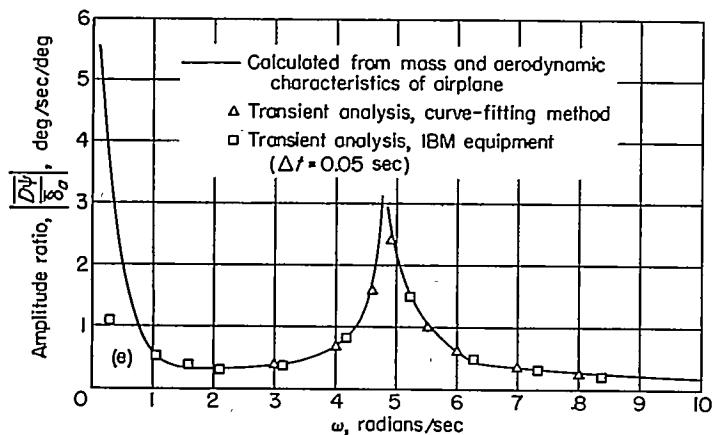
(e) Amplitude ratio $\frac{D\psi}{\delta_a}$.

FIGURE 8.—Continued.

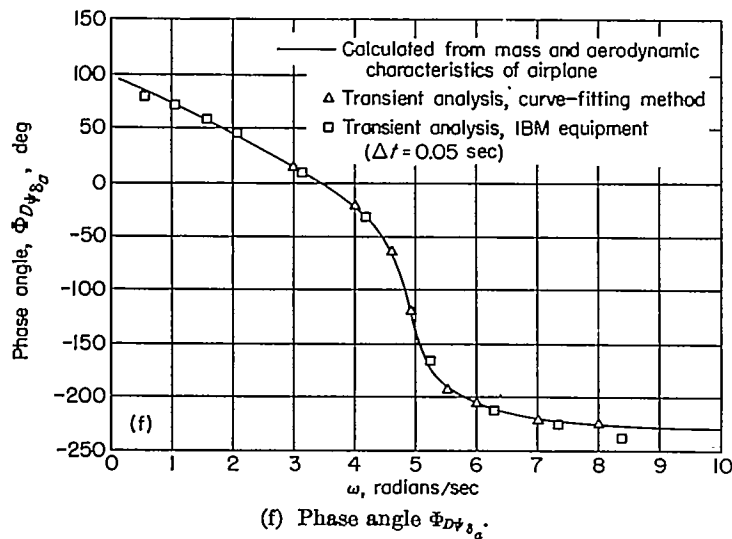
(f) Phase angle $\Phi_{D\psi/\delta_a}$.

FIGURE 8.—Concluded.

good accuracy cannot be eliminated as it was in the body of the report when the equations were separated.

A comparison of the values of the derivatives based on frequency responses obtained by the curve-fitting method and obtained from the two methods of treating the equations of motion indicates very good agreement for all the parameters except C_{l_r} . The poor agreement for C_{l_r} is felt

TABLE XII.—COMPARISON BETWEEN STABILITY DERIVATIVES USED IN CALCULATION OF TRANSIENTS AND THOSE DERIVED FROM TRANSIENTS FOR EXAMPLE IN APPENDIX B

| Derivative | Assumed value | Transient analysis, curve-fitting method | | Transient analysis, IBM equipment | |
|--------------------|---------------|--|------------------------------------|-----------------------------------|------------------------------------|
| | | From eqs. of present report | From eqs. of motion as vector eqs. | From eqs. of present report | From eqs. of motion as vector eqs. |
| C_{l_r} | -0.400 | -0.378 | -0.397 | -0.388 | -0.391 |
| C_{l_p} | 0.080 | 0.0882 | 0.110 | 0.130 | 0.099 |
| $C_{l_{\dot{p}}}$ | -0.126 | -0.127 | -0.134 | -0.129 | -0.128 |
| $C_{l_{\ddot{p}}}$ | -0.100 | -0.100 | -0.100 | -0.098 | -0.099 |
| C_{n_r} | -0.020 | -0.020 | -0.021 | -0.029 | -0.025 |
| C_{n_p} | -0.400 | -0.382 | -0.397 | -0.786 | -0.646 |
| $C_{n_{\dot{p}}}$ | 0.250 | 0.253 | 0.257 | 0.213 | 0.258 |
| $C_{n_{\ddot{p}}}$ | -1.000 | -1.050 | -1.003 | -0.600 | 1.260 |

not to be significant since C_{l_r} generally makes a negligible contribution to the lateral motions of an airplane and is important only in the lightly damped spiral mode of motion which is very difficult to define accurately from a transient response.

A similar comparison of the two sets of values based on frequency responses obtained with the IBM equipment shows good agreement except for the derivatives C_{l_r} , C_{n_r} , and C_{r_p} . The poor agreement between the initially assumed values of C_{l_r} , C_{n_r} , and C_{r_p} and those calculated from the frequency responses obtained with the IBM equipment is probably due partly to the fact that data were not obtained for frequencies near the natural frequency of the airplane with the particular routine used for the IBM equipment and partly to small inaccuracies that exist in the data at the frequencies that were included. These small inaccuracies undoubtedly could have been reduced somewhat by the use of a smaller time interval in the numerical integrations performed by the IBM equipment.

The use of the frequency-response data which were obtained from the transient responses by the curve-fitting method and which included frequencies near the natural frequency of the airplane resulted in good agreement for these derivatives. Therefore, it appears that further investigation into the effects of the choice of the frequency range to be used in extracting stability derivatives from the frequency-response data is warranted.

APPENDIX C

LEAST-SQUARES VECTOR SOLUTION OF THE EQUATIONS OF LATERAL MOTION

Some of the results shown in table XII were obtained by applying the method of reference 4 to the lateral equations of motion (appendix B). The important details of this method are illustrated in this appendix by applying them to equation (1) which is

$$D\beta + K_1\beta - K_2\phi + D\psi = F_1[\delta_r(t)] \quad (C1)$$

If the flight data are expressed in frequency-response form, that is for every frequency ω there is an amplitude ratio and a phase-angle relationship, then the lateral variables can be considered to be constant-amplitude vectors rotating in the complex plane with fixed phase relationships for any given frequency. Equation (C1) can be expressed as

$$\left(\frac{D\beta}{\delta_r}\right)_j + K_1\left(\frac{\beta}{\delta_r}\right)_j - K_2\left(\frac{\phi}{\delta_r}\right)_j + \left(\frac{D\psi}{\delta_r}\right)_j - F_1 = v_j \quad (j = \omega_1, \omega_2, \dots, \omega_n) \quad (C2)$$

where $\left(\frac{D\beta}{\delta_r}\right)_j$, $\left(\frac{\beta}{\delta_r}\right)_j$, $\left(\frac{\phi}{\delta_r}\right)_j$, $\left(\frac{D\psi}{\delta_r}\right)_j$ are the airplane frequency responses expressed in vector form, and the residual v , is a vector at each frequency. In this treatment K_2 is assumed to be known and the most probable values of the unknowns K_1 and F_1 are such as to make the sum of the squares of the residual a minimum; that is, $\sum_{j=\omega_1}^{\omega_n} (v_j)^2$ is equal to a minimum. The square of the residual vector is obtained from the scalar or dot product of the two vectors, namely,

$$v_j \cdot v_j = (v_j)^2 \quad (C3)$$

The values of K_1 and F_1 which satisfy the condition that $\sum_{j=\omega_1}^{\omega_n} (v_j)^2$ be a minimum are obtained from a simultaneous solution of the equations

$$\frac{\partial}{\partial K_1} \sum_{j=\omega_1}^{\omega_n} (v_j \cdot v_j) = 0 \quad (C4)$$

$$\frac{\partial}{\partial F_1} \sum_{j=\omega_1}^{\omega_n} (v_j \cdot v_j) = 0 \quad (C5)$$

These equations after expansion are written in matrix form as follows:

(a) For the sideslipping motion

$$\begin{bmatrix} n & \sum_{j=\omega_1}^{\omega_n} (-A_\beta)_j \\ \sum_{j=\omega_1}^{\omega_n} (-A_\beta)_j & \sum_{j=\omega_1}^{\omega_n} \left(\left|\frac{\beta}{\delta_r}\right|\right)_j^2 \end{bmatrix} \begin{Bmatrix} F_1 \\ K_1 \end{Bmatrix} = \begin{Bmatrix} \sum_{j=\omega_1}^{\omega_n} (-\omega B_\beta - \omega B_\psi - K_2 A_\phi)_j \\ \sum_{j=\omega_1}^{\omega_n} [\omega(A_\beta B_\psi - B_\beta A_\psi) + K_2(A_\beta A_\phi + B_\beta B_\phi)]_j \end{Bmatrix} \quad (C6)$$

(b) For the rolling motion

$$\begin{bmatrix} n & \sum_{j=\omega_1}^{\omega_n} (-A_\beta)_j & \sum_{j=\omega_1}^{\omega_n} (\omega B_\phi)_j & \sum_{j=\omega_1}^{\omega_n} (-\omega B_\psi)_j \\ \sum_{j=\omega_1}^{\omega_n} (-A_\beta)_j & \sum_{j=\omega_1}^{\omega_n} \left(\left|\frac{\beta}{\delta_r}\right|\right)_j^2 & \sum_{j=\omega_1}^{\omega_n} \omega_j (-A_\beta B_\phi + A_\phi B_\beta)_j & \sum_{j=\omega_1}^{\omega_n} \omega_j (A_\beta B_\psi - A_\psi B_\beta)_j \\ \sum_{j=\omega_1}^{\omega_n} (\omega B_\phi)_j & \sum_{j=\omega_1}^{\omega_n} \omega_j (-A_\beta B_\phi + A_\phi B_\beta)_j & \sum_{j=\omega_1}^{\omega_n} \left(\omega_j^2 \left|\frac{\phi}{\delta_r}\right|\right)_j & \sum_{j=\omega_1}^{\omega_n} -\omega_j^2 (A_\phi A_\psi + B_\phi B_\psi)_j \\ \sum_{j=\omega_1}^{\omega_n} (-\omega B_\psi)_j & \sum_{j=\omega_1}^{\omega_n} \omega_j (A_\beta B_\psi - A_\psi B_\beta)_j & \sum_{j=\omega_1}^{\omega_n} -\omega_j^2 (A_\phi A_\psi + B_\phi B_\psi)_j & \sum_{j=\omega_1}^{\omega_n} \left(\omega_j^2 \left|\frac{\psi}{\delta_r}\right|\right)_j \end{bmatrix} \begin{Bmatrix} F_2 \\ K_3 \\ K_4 \\ K_5 \end{Bmatrix} = \begin{Bmatrix} \sum_{j=\omega_1}^{\omega_n} \omega_j^2 (-A_\phi + K_5 A_\psi)_j \\ \sum_{j=\omega_1}^{\omega_n} \omega_j^2 (A_\beta A_\phi + B_\beta B_\phi - K_5 A_\beta A_\psi - K_5 B_\beta B_\psi)_j \\ \sum_{j=\omega_1}^{\omega_n} K_5 \omega_j^3 (A_\psi B_\phi - B_\psi A_\phi)_j \\ \sum_{j=\omega_1}^{\omega_n} \omega_j^3 (A_\phi B_\psi - A_\psi B_\phi)_j \end{Bmatrix} \quad (C7)$$

(c) For the yawing motion

$$\begin{bmatrix}
 n & \sum_{j=\omega_1}^{\omega_n} (A_\beta)_j & \sum_{j=\omega_1}^{\omega_n} (-\omega B_\phi)_j & \sum_{j=\omega_1}^{\omega_n} (\omega B_\psi)_j \\
 \sum_{j=\omega_1}^{\omega_n} (A_\beta)_j & \sum_{j=\omega_1}^{\omega_n} \left(\left| \frac{\bar{\beta}}{\delta_r} \right|^2 \right)_j & \sum_{j=\omega_1}^{\omega_n} \omega_j (-A_\beta B_\phi + A_\phi B_\beta)_j & \sum_{j=\omega_1}^{\omega_n} \omega_j (A_\beta B_\psi - A_\psi B_\beta)_j \\
 \sum_{j=\omega_1}^{\omega_n} (-\omega B_\phi)_j & \sum_{j=\omega_1}^{\omega_n} \omega_j (-A_\beta B_\phi + A_\phi B_\beta)_j & \sum_{j=\omega_1}^{\omega_n} \left(\omega^2 \left| \frac{\bar{\phi}}{\delta_r} \right|^2 \right)_j & \sum_{j=\omega_1}^{\omega_n} -\omega_j^2 (A_\phi A_\psi + B_\phi B_\psi)_j \\
 \sum_{j=\omega_1}^{\omega_n} (\omega B_\psi)_j & \sum_{j=\omega_1}^{\omega_n} \omega_j (A_\beta B_\psi - A_\psi B_\beta)_j & \sum_{j=\omega_1}^{\omega_n} -\omega_j^2 (A_\phi A_\psi + B_\phi B_\psi)_j & \sum_{j=\omega_1}^{\omega_n} \left(\omega^2 \left| \frac{\bar{\psi}}{\delta_r} \right|^2 \right)_j
 \end{bmatrix}
 \begin{Bmatrix}
 F_3 \\
 K_7 \\
 K_9 \\
 K_{10}
 \end{Bmatrix}
 =
 \begin{Bmatrix}
 \sum_{j=\omega_1}^{\omega_n} \omega_j^2 (-A_\psi + K_8 A_\phi)_j \\
 \sum_{j=\omega_1}^{\omega_n} \omega_j^2 (-A_\beta A_\psi - B_\beta B_\psi + K_8 A_\beta A_\phi + K_8 B_\beta B_\phi)_j \\
 \sum_{j=\omega_1}^{\omega_n} \omega_j^3 (-A_\phi B_\psi + A_\psi B_\phi)_j \\
 \sum_{j=\omega_1}^{\omega_n} K_8 \omega_j^3 (A_\phi B_\psi - B_\phi A_\psi)_j
 \end{Bmatrix} \quad (C8)$$

where n is the number of frequency points and the definitions of A_β , B_β , A_ψ , B_ψ , A_ϕ , and B_ϕ are given in equations (8) and (9).

REFERENCES

1. Donegan, James J., and Pearson, Henry A.: Matrix Method of Determining the Longitudinal-Stability Coefficients and Frequency Response of an Aircraft From Transient Flight Data. NACA Rep. 1070, 1952. (Supersedes NACA TN 2370.)
2. Donegan, James J.: Matrix Methods for Determining the Longitudinal-Stability Derivatives of an Airplane From Transient Flight Data. NACA Rep. 1169, 1954. (Supersedes NACA TN 2902.)
3. Campbell, G. F., Whitecomb, D. W., and Breuhaus, W. O.: Dynamic Longitudinal Stability and Control Flight Tests of a B-25J Airplane. Forced Oscillation and Step Function Response Methods, Utilizing an A-12 Automatic Pilot. Rep. No. TB-405-F-3, Cornell Aero. Lab., Inc., Apr. 15, 1947.
4. Schumacher, Lloyd E.: A Method for Evaluating Aircraft Stability Parameters From Flight Test Data. USAF Tech. Rep. No. WADC-TR-52-71, Wright Air Dev. Center, U. S. Air Force, June 1952.
5. Mueller, R. K.: The Graphical Solution of Stability Problems. Jour. Aero. Sci., vol. 4, no. 8, June 1937, pp. 324-331.
6. Segel, L.: Dynamic Lateral Stability Flight Tests of an F-80A Airplane by the Forced Oscillation and Step Function Response Methods. USAF Tech. Rep. No. 5996 (Cornell Aero. Lab., Inc. Contract Nos. W33-038-ac-17003 and W33-038-ac-18517; E. O. Nos. 458-414 and 451-341), Air Materiel Command, U. S. Air Force, Sept. 1950.
7. Swanson, Robert S., and Mastrocola, N.: Survey of Methods for Determining Stability Derivatives in Free Flight. U. S. Naval Air Missile Test Center (Pt. Mugu, Calif.), Aug. 2, 1948.
8. Eggleston, John M., and Mathews, Charles W.: Application of Several Methods for Determining Transfer Functions and Frequency Response of Aircraft From Flight Data. NACA Rep. 1204, 1954. (Supersedes NACA TN 2997.)
9. Milne, William Edmund: Numerical Calculus. Princeton Univ. Press, 1949.

1

2

3

4

5

6

7

8

9

10

11

12

13

14

15

16

17

18

19

20

21

22

23

24

25

26

27

28

29

30

31

32

33

34

35

36

37

38

39

40

41

42

43

44

45

46

47

48

49

50

51

52

53

54

55

56

57

58

59

60

61

62

63

64

65

66

67

68

69

70

71

72

73

74

75

76

77

78

79

80

81

82

83

84

85

86

87

88

89

90

91

92

93

94

95

96

97

98

99

100

101

102

103

104

105

106

107

108

109

110

111

112

113

114

115

116

117

118

119

120

121

122

123

124

125

126

127

128

129

130

131

132

133

134

135

136

137

138

139

140

141

142

143

144

145

146

147

148

149

150

151

152

153

154

155

156

157

158

159

160

161

162

163

164

165

166

167

168

169

170

171

172

173

174

175

176

177

178

179

180

181

182

183

184

185

186

187

188

189

190

191

192

193

194

195

196

197

198

199

200

201

202

203

204

205

206

207

208

209

210

211

212

213

214

215

216

217

218

219

220

221

222

223

224

225

226

227

228

229

230

231

232

233

234

235

236

237

238

239

240

241

242

243

244

245

246

247

248

249

250

251

252

253

254

255

256

257

258

259

260

261

262

263

264

265

266

267

268

269

270

271

272

273

274

275

276

277

278

279

280

281

282

283

284

285

286

287

288

289

290

291

292

293

294

295

296

297

298

299

300

301

302

303

304

305

306

307

308

309

310

311

312

313

314

315

316

317

318

319

320

321

322

323

324

325

326

327

328

329

330